JOURNAL OF VIROLOGY, May 2008, p. 4384–4399 Vol. 82, No. 9
0022-538X/08/$08.00+0 doi:10.1128/JVI.01953-07

Dominant Negative Inhibition of Human Immunodeficiency Virus Particle Production by the Nonmyristoylated Form of Gag▽

Shigeo Kawada,[1]† Toshiyuki Goto,[2] Hiyori Haraguchi,[1] Akira Ono,[3] and Yuko Morikawa[1]*

Kitasato Institute for Life Sciences and Graduate School for Infection Control, Kitasato University, Shirokane 5-9-1, Minato-ku, Tokyo 108-8641, Japan[1]; School of Health Science, Faculty of Medicine, Kyoto University, Kawaraha-cho 53, Shogoin, Sakyo-ku, Kyoto 606-8507, Japan[2]; and Department of Microbiology and Immunology, University of Michigan Medical School, Ann Arbor, Michigan 48109[3]

Received 6 September 2007/Accepted 19 February 2008

Myristoylation of human immunodeficiency virus (HIV) Gag protein is essential for membrane targeting of Gag and production of viral particles. We show here that coexpression of wild-type and nonmyristoylated forms of HIV Gag resulted in severe inhibition of viral particle production, indicating that the nonmyristoylated counterpart had a dominant negative effect on particle release. When coexpressed, the nonmyristoylated Gag partially incorporated into membrane and lipid raft fractions, likely through coassembly with the wild-type Gag. The membrane and raft associations of the wild-type Gag appeared unaffected, and yet particle production was severely impaired. When viral particles produced from the coexpressing cells were analyzed, the wild-type Gag was more abundant than the nonmyristoylated Gag. Confocal microscopy showed that both forms of Gag were diffusely distributed in the cytoplasm of coexpressing cells but that a portion of the wild-type Gag population was accumulated in EEA1- and CD63-positive endosomes. The intracellular accumulation of Gag was more frequently observed at late time points. The Gag accumulation was also observed on the cell surface protrusion. Electron microscopy of the coexpressing cells revealed budding arrest phenotypes, including the occurrence of interconnected virions on the plasma membrane, and intracellular budding. We also show that the inhibition of particle production and the Gag accumulation to endosomes were suppressed when the nucleocapsid (NC) domain was deleted from the nonmyristoylated Gag, although the NC-deleted Gag was still capable of coassembly. Overall, our data indicate that coassembly with the nonmyristoylated Gag impairs HIV particle release, a phenomenon that may involve NC-mediated Gag-Gag interaction.

The retroviral Gag protein, the main structural component of the viral particle, directs particle assembly. The Gag protein contains several functionally and structurally distinct domains: the matrix (MA) domain at the N-terminal region of Gag, responsible for association with membrane (10, 25, 40, 57); the capsid (CA) domain at the central region, essential for Gag-Gag interaction (7, 18, 20, 21, 56, 67); and the nucleocapsid (NC) domain near the C-terminal region, absolutely required for viral genome packaging and important for Gag multimerization (6, 13, 59, 68). Another Gag region that is necessary for pinching off viral particles, the late (L) domain, has also been identified in some retroviruses (24, 70). Recent studies have identified host factors that bind to the L domain and are responsible for particle budding, one of which is tumor susceptibility gene 101 (TSG101), a molecule in the endosomal sorting machinery (14, 18, 36, 66).

The Gag protein is synthesized in the cytosol and targeted to the plasma membrane where particle budding occurs. Most mammalian retroviral Gag proteins, including human immunodeficiency virus (HIV) Gag, are modified at the N-terminal glycine by myristic acid, which is a key player for tight membrane association (71). A number of studies have shown the essential role of N-terminal myristoylation in Gag targeting to the plasma membrane. For example, the nonmyristoylated Gag protein obtained by amino acid substitution at the N-terminal glycine fails to target to the plasma membrane and produces no virus particles (10, 25, 23). The use of myristoylation inhibitors, such as analogues of myristic acid and myristoyl-glycine, also produces nonmyristoylated Gag and leads to a severe reduction in infectious particle production, suggesting an effective antivirus therapeutic strategy (11, 32, 35, 58, 65).

For type C retroviruses and lentiviruses, Gag assembly to virus particles occurs after Gag targeting to the plasma membrane. Although membrane binding of Gag may promote its multimerization, the Gag-Gag interaction can take place without membrane binding of Gag. Consistent with this notion, previous studies have shown that nonmyristoylated Gag incorporates into viral particles when it coexists with myristoylated Gag (12, 37, 44, 52), indicating that nonmyristoylated Gag is capable of coassembly with wild-type Gag to form viral particles. However, some studies have reported that C-terminal truncations of Gag assembly domains result in a decrease in Gag multimerization and membrane affinity, suggesting that the membrane affinity of Gag is enhanced by its multimerization (60, 72). This idea has been supported by a recent study in which the myristoyl moiety at the N terminus was exposed in a MA trimer but sequestered in a MA monomer. The study has also suggested that Gag assembly may be promoted by intermolecular interactions of the exposed myristoyl moiety (64). If intermolecular interactions of the myristoyl moiety were im-

* Corresponding author. Mailing address: Kitasato Institute for Life Sciences and Graduate School for Infection Control, Kitasato University, Shirokane 5-9-1, Minato-ku, Tokyo 108-8641, Japan. Phone: 81-3-5791-6129. Fax: 81-3-5791-6268. E-mail: morikawa@lisci.kitasato-u.ac.jp.

† Present address: The University of Tokyo, Kashiwa-no-ha 5-1-5, Kashiwa, Chiba 277-8561, Japan.

▽ Published ahead of print on 27 February 2008.

portant for Gag assembly, a defect of particle assembly would occur if a portion of the Gag population were to be nonmyristoylated. A more general question would address what impact the nonmyristoylated Gag incorporated into the Gag assembly complex has on the membrane affinity of the Gag complex, Gag localization, and virus particle budding and release. To address these questions, we distinguished between myristoylated (wild-type) Gag and nonmyristoylated Gag of HIV by adding a distinct epitope tag at each C terminus and carrying out coexpression experiments. Our data indicate that the nonmyristoylated Gag does not affect the membrane binding of the Gag complex but imposes a severe dominant negative effect on particle production through particle budding arrest and Gag relocation.

MATERIALS AND METHODS

Construction of HIV-1 molecular clones. HIV type 1 (HIV-1) proviral molecular clone pNL43 (1) was used to construct its derivatives. For nonmyristoylated Gag protein, replacement of the N-terminal glycine with alanine was carried out by overlapping PCR using a forward primer, 5′-GAAGGAGAGAGATGGCTGCGAGAGCGTCGG-3′, and its complementary oligonucleotide. The Gag mutant with deletion of the NC domain (i.e., of all but seven amino acids of the NC) was described elsewhere (50), as was the Gag with multiple amino acid substitutions of the PTAP sequence in the p6 domain (15). Molecular clones expressing Gag protein tagged with a Flag or hemagglutinin (HA) epitope sequence at the C terminus were constructed in this study, and similar constructs were described previously (48). In brief, the *gag* gene (truncated just before the termination codon) was amplified by PCR using a reverse primer containing the Flag or HA epitope tag sequence 5′-GGCCTGGCCATTACTTATCGTCGTCATCCTTGTAATCTTGTGACGAGGGGTCGCTGCCAAAGAG-3′ or 5′-GGCCTGGCCATTAAGCGTAATCTGGAACATCGTATGGGTATTGTGACGAGGGGTCGCTGCCAAAGAG-3′, respectively (the underlined section is a BalI linker), and substituted for the wild-type or nonmyristoylated form of the *gag* gene of pNL43. When the substitution was carried out, the *pol* gene region from nucleotide position 2290 (the end of the *gag* gene) to 4553 (located in the integrase gene) was deleted by the use of the BalI sites in the *pol* gene. Accordingly, the constructs produced uncleaved Gag protein tagged with Flag or HA epitope but no *pol* gene products.

Cell culture and DNA transfection. HeLa cells were grown in Eagle's minimum essential medium supplemented with 10% fetal bovine serum. Transfection with plasmid DNA was carried out using Lipofectamine 2000 (Invitrogen).

Purification of HIV particles. Purification of viral particles was carried out by the standard procedures. At 2 days posttransfection, the culture media of cells were clarified, filtered, and centrifuged through 20% (wt/vol) sucrose cushions in an SW55 rotor (Beckman Coulter) at 32,000 rpm for 1.5 h at 4°C. The HIV particle pellets were resuspended with phosphate-buffered saline (PBS).

Membrane and lipid raft flotation centrifugation. Equilibrium flotation centrifugation with membranes was performed as described previously (45, 51). Cells were harvested at 2 days posttransfection and resuspended in buffer A (50 mM Tris [pH 8.0], 1 mM EDTA, and 1 mM dithiothreitol) containing 150 mM NaCl. Following brief sonication, the cell lysates were clarified at 2,000 rpm for 5 min at 4°C. The supernatants were adjusted to 70% (wt/vol) sucrose, layered at the bottom of 70%, 65%, and 10% (wt/vol) sucrose step gradients in PBS, and subjected to equilibrium flotation centrifugation. Centrifugation was performed in an SW55 rotor apparatus at 4°C at 32,000 rpm overnight. For lipid raft flotation experiments, cell lysates were treated after sonication at 4°C with 0.5% Triton X-100 for 10 min and clarified. The supernatants were similarly separated in 70%, 65%, and 10% (wt/vol) sucrose step gradients. In some experiments, cells were resuspended in buffer A containing 500 mM NaCl and, following sonication, the supernatants were similarly subjected to equilibrium flotation centrifugation.

Western blotting. Cells and viral particles were collected at 2 days posttransfection and subjected to sodium dodecyl sulfate-polyacrylamide gel electrophoresis (SDS-PAGE). Western blotting was carried out using anti-Flag mouse monoclonal antibody (M2; Sigma), anti-HA rabbit antibody (Santa Cruz), anti-HIV-1 p24CA mouse monoclonal antibody (Advanced Biotechnologies), anti-HIV-1 gp120Env sheep antibody (Medical Research Council AIDS Reagent Repository, United Kingdom), or antiactin mouse monoclonal antibody (Sigma).

Immunofluorescent staining and confocal microscopy. HeLa cells were subjected to immunofluorescent analysis at 2 days posttransfection unless otherwise indicated. Cells were fixed with 3.7% paraformaldehyde in PBS for 30 min at room temperature and were treated with 0.1% Triton X-100 for 5 min at room temperature for membrane permeabilization. Following blocking with 1% bovine serum albumin in PBS, cells were incubated with primary antibodies and subsequently with secondary antibodies conjugated with Alexa Fluor (Molecular Probes). For nuclear staining, cells were further incubated with TOPRO-3 (Molecular Probes). In some experiments, cells were incubated with epidermal growth factor (EGF)-Texas Red (Molecular Probes) or transferrin (Trf)-Alexa Fluor 568 (Molecular Probes) at 37°C for 15 to 20 min before paraformaldehyde fixation. The following reagents were used for this study: anti-Flag mouse monoclonal antibody (Sigma), anti-HA rabbit antibody (Santa Cruz), anti-TGN46 sheep antibody (Serotec), anti-EEA1 mouse monoclonal antibody (BD Transduction Laboratories), anti-Rab7 rabbit antibody (Santa Cruz), anti-LAMP1 mouse monoclonal antibody (Santa Cruz), anti-CD63 rabbit antibody (Santa Cruz), and EGF-Texas Red, Trf-Alexa Fluor 568, anti-mouse immunoglobulin G-Alexa Fluor (IgG-Alexa Fluor) 488 and 568, anti-rabbit IgG-Alexa Fluor 488 and 568, and anti-sheep IgG-Alexa Fluor 568 (Molecular Probes). After staining, the cells were mounted with antibleaching reagent and observed with a laser scanning microscope (Leica).

Electron microscopy. At 2 days posttransfection, the cells were fixed in 2% glutaraldehyde–100 mM cacodylate buffer (pH 7.2) and postfixed with 1% osmium tetroxide. Electron microscopic observation was performed by the standard procedures.

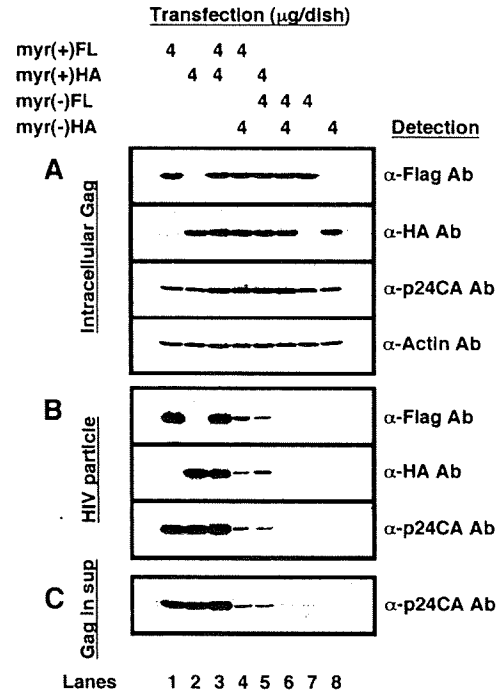

FIG. 1. Intracellular expression of Gag and production of viral particles. HeLa cells (in 6-cm-diameter dishes) were transfected with myr(+)Gag and/or myr(−)Gag constructs of the HIV-1 molecular clone pNL43. The DNA amounts of the Gag constructs used [myr(+)Gag-Flag, myr(+)Gag-HA, myr(−)Gag-Flag, and myr(−)Gag-HA] are indicated at the top of the panel. Two days posttransfection, cells were collected (A), and culture media were subjected to purification of viral particles by ultracentrifugation (B) or trichloroacetic acid precipitation (C). The materials were subjected to SDS-PAGE followed by Western blotting using anti-Flag, anti-HA, anti-HIV-1 p24CA, and antiactin antibodies (Ab). FL, Flag.

RESULTS

Inhibition of HIV particle production by coexpression of nonmyristoylated Gag. To distinguish between the myristoylated (wild-type) and nonmyristoylated forms of HIV Gag, we added a Flag epitope tag to the C terminus of the wild-type Gag [referred to as myr(+)Gag-Flag] and an HA epitope tag to that of the

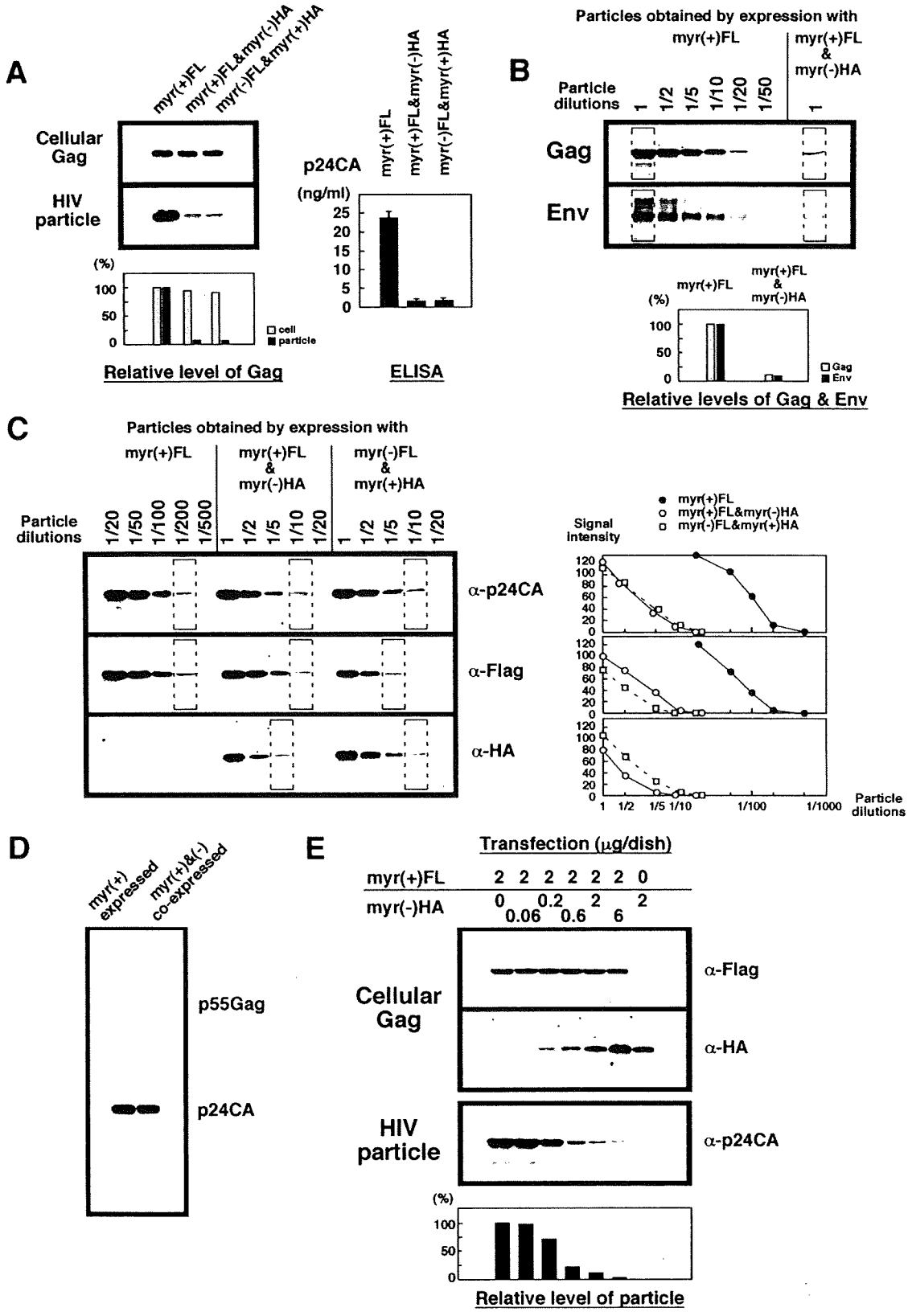

FIG. 2. Dominant negative inhibition of viral particle production by coexpression with nonmyristoylated Gag. (A) Quantitation of viral particle yields. HeLa cells (in 6-cm-diameter dishes) were transfected with myr(+)Gag-Flag (8 μg) alone or cotransfected with a combination of myr(+)Gag-Flag (4 μg) and myr(−)Gag-HA (4 μg) molecular clones or with a reverse combination of the myr(+)Gag-HA (4 μg) and myr(−)Gag-Flag (4 μg) molecular clones. At 2 days posttransfection, the cells were collected and viral particles were purified by ultracentrifugation and resuspended in PBS. Equivalent

nonmyristoylated Gag [referred to as myr(−)Gag-HA], respectively. Reverse tagging of Gag constructs was also carried out to produce myr(+)Gag-HA and myr(−)Gag-Flag. These Gag constructs were introduced into the *pol*-deleted form of molecular clone pNL43 (1). Following transfection into HeLa cells, intracellular Gag antigens were examined by Western blotting using anti-Flag, anti-HA, and anti-HIV-1 p24CA antibody (Fig. 1A). As expected, anti-Flag antibody was reactive in myr(+)Gag-Flag- and myr(−)Gag-Flag-transfected cells, while anti-HA antibody was reactive in myr(−)Gag-HA- and myr(+)Gag-HA-transfected cells. Accordingly, both antibodies were reactive in cells cotransfected with a combination of the Flag-tagged and HA-tagged Gag constructs. Western blotting using anti-p24CA antibody revealed that the total expression levels of Gag proteins in doubly transfected cells were higher than those in singly transfected cells (Fig. 1A, lanes 3 to 6), while the expression levels of actin assessed as an internal control were broadly equivalent.

Culture media of the cells were harvested, and following clarification, the HIV particles were pelleted down through sucrose cushions (Fig. 1B). Western blotting confirmed that the myr(+)Gag constructs, whether tagged with Flag or HA, produced particles (Fig. 1B, lanes 1 to 3), whereas the myr(−)Gag constructs did not (Fig. 1B, lanes 6 to 8). Particles released by cells cotransfected with myr(+)Gag-Flag and myr(+)Gag-HA showed strong signals for both antibodies (Fig. 1B, lane 3). In contrast, particles purified from cells cotransfected with myr(+)Gag and myr(−)Gag constructs, although they were reactive with both anti-Flag and anti-HA antibodies, showed only a trace of Gag molecules, even when equal volumes of the particle fractions were used (Fig. 1B, lanes 4 and 5). These results indicated that the nonmyristoylated Gag was incorporated into viral particles through coassembly with the myristoylated Gag and that the efficiency of particle production from the coexpressing cells was much lower than that from cells expressing the myristoylated Gag alone. The latter was evident when Western blotting was carried out using anti-p24CA antibody and indicated that particle production was inhibited by coexpression with the nonmyristoylated Gag. When clarified culture media were analyzed by Western blotting, the pattern of the band intensity was similar to that shown for the purified particle fractions, indicating little or no release of virion-free Gag molecules (Fig. 1C).

The Western blots of cells and viral particles probed with anti-p24CA antibody were subjected to semiquantitation. Intracellular levels of Gag were broadly equivalent, whereas particle yields were reduced to 5 to 10% of the former levels (Fig. 2A, left). The particle yields were quantitated using p24CA antigen capture enzyme-lined immunosorbent assay (ELISA). Quantitation by p24CA antigen capture ELISA indicated that coexpression with the nonmyristoylated Gag, regardless of the combination of constructs used, reduced the particle yields to 5 to 10% of the former levels (as assessed by four independent experiments) (Fig. 2A, right panel). For additional semiquantitation by Western blotting, the purified particle fractions were serially diluted (up to 50-fold) and were compared with the fraction obtained by transfection with the myristoylated Gag alone. When probed with anti-p24CA antibody, the particle yield obtained by coexpression with the nonmyristoylated Gag was found to be approximately 10- to 20-fold lower than that obtained by single expression of the myristoylated Gag. When probed with anti-gp120Env antibody, the particle yield obtained by the coexpression similarly appeared to be 10- to 20-fold lower, indicating that the incorporation of HIV Env protein into viral particles was unaffected (Fig. 2B, upper panel). The data were confirmed when the band intensity of undiluted fractions was semiquantitated (Fig. 2B, lower panel).

The results shown in Fig. 1B suggested slightly selective incorporation of myr(+)Gag molecules into viral particles. To examine this point further, we carried out semiquantitative Western blotting using purified particle fractions. Cells were cotransfected with myr(+)Gag-Flag and myr(−)Gag-HA or with myr(+)Gag-HA and myr(−)Gag-Flag. Following purification of HIV particles, the particle fractions were serially diluted [up to 500-fold in the case of the myr(+) form alone; up to 20-fold in the case of myr(+) plus myr(−) forms] and subjected to Western blotting, and the endpoint dilutions were compared. Western blotting using anti-p24CA antibody (to determine the level of total Gag proteins) showed that the coexpressing cells produced a 20-fold lower particle yield, regardless of the combination of constructs used, than the cells expressing the myristoylated Gag alone [the endpoints were at 200-fold dilution for the myr(+) form alone and at 10-fold dilution for the myr(+) plus myr(−) forms] (Fig. 2C, top panel, left). When the same series of dilutions of the particle fractions were probed with anti-Flag antibody, it was

volumes of samples were analyzed by Western blotting using anti-HIV-1 p24CA antibody. Data were semiquantitated by use of an image analyzer, and the levels of Gag in single expression of myr(+)Gag-Flag were set at 100% (left panel). Particle yields were measured by p24CA antigen capture ELISA (right panel). (B) Env incorporation into viral particles. Transfection and particle purification were carried out as described for panel A. Particle fractions were serially diluted up to 50-fold and were subjected to Western blotting using anti-HIV-1 p24CA and anti-gp120Env antibodies. Data of undiluted fractions (marked) represent the results of semiquantitation experiments. (C) Efficiency of incorporation of myr(+)Gag and myr(−)Gag into viral particles. Transfection and particle purification were carried out as described for panel A. Each of the purified particle fractions was serially diluted and subjected to Western blotting using anti-HIV-1 p24CA, anti-Flag, and anti-HA antibodies. An endpoint is marked for each sample dilution (left panel). Data were semiquantitated by use of an image analyzer (right panel). (D) Efficiency of Gag processing. HeLa cells were transfected with 8 μg of the wild-type pNL43 or a mixture of 4 μg of the wild-type pNL43 and 4 μg of its derivative containing myr(−) mutation, both of which contained active HIV protease. Viral particles were collected and resuspended in PBS. An approximately 20-fold-larger volume of the cotransfection sample was loaded on a gel and compared with the wild-type sample. Detection was carried out by Western blotting using anti-HIV-1 p24CA antibody. (E) Dose-dependent inhibition of viral particle production. HeLa cells were cotransfected at various DNA ratios of myr(+)Gag-Flag and myr(−)Gag-HA constructs, which were made by a combination of a fixed amount of DNA for myr(+)Gag-Flag (2 μg) and increasing amounts (0, 0.06, 0.2, 0.6, 2, and 6 μg) of DNA for myr(−)Gag-HA. Total DNA amounts were normalized to 8 μg with pUC plasmid. Viral particles were collected as described above. Cells were subjected to Western blotting using anti-Flag and anti-HA antibodies. Equivalent volumes of all particle samples were analyzed by Western blotting using anti-HIV-1 p24CA antibody, and data were semiquantitated. The particle yield produced by single expression of myr(+)Gag-Flag was set at 100%.

found that myr(+)Gag-Flag was incorporated into particles approximately 2-fold more efficiently than myr(−)Gag-Flag [the endpoints were at 10-fold dilution for the myr(+)FL plus myr(−)HA forms and at 5-fold dilution for the myr(−)FL plus myr(+)HA forms] (Fig. 2C, middle panel, left), suggesting that myristoylated Gag was preferentially incorporated into viral particles. Western blotting using anti-HA antibody confirmed these findings (Fig. 2C, bottom panel, left). The preferential incorporation of myristoylated Gag was confirmed when the Western blots probed by anti-Flag and anti-HA antibodies were subjected to semiquantitation (Fig. 2C, right panel). Preferential incorporation of myristoylated Gag has been also reported for murine leukemia virus (4).

The efficiency of Gag processing was examined using the wild-type pNL43 construct and its nonmyristoylated counterpart, both of which contained active HIV protease. Transfection of DNA and purification of HIV particles were carried out as before. The levels of particle production were assessed by Western blotting and by antigen capture ELISA (data not shown). When equivalent levels of Gag antigens were analyzed by Western blotting, p24CA, but not p55Gag, was seen in both samples (wild-type form alone versus wild-type plus nonmyristoylated forms), indicating that Gag was fully processed even when coexpressed with the nonmyristoylated form (Fig. 2D).

The experiments described above were carried out by equimolar cotransfection of the myristoylated and nonmyristoylated Gag constructs. To test whether the inhibition of particle production was affected by the expression levels of the nonmyristoylated Gag, cotransfection experiments were carried out in which the amount of DNA for the myristoylated Gag was fixed whereas that of DNA for the nonmyristoylated Gag was adjusted. Western blotting using anti-Flag and anti-HA antibodies confirmed that the expression levels of myr(+)Gag-Flag in the cells were constant whereas those of myr(−)Gag-HA increased in a DNA dose-dependent manner (Fig. 2E, top panel), suggesting that the total amount of DNA used for each transfection was not beyond the maximum expression level in the cells. The HIV particles present in culture media were collected by centrifugation through sucrose cushions and analyzed. Western blotting using anti-p24CA antibody showed dose-dependent inhibition of HIV particle production (Fig. 2E, middle panel). When the Western blot of viral particles was semiquantitated, a three- to fourfold decrease of particle production was observed even at the myr(+)Gag-to-myr(−)Gag DNA ratio of 2:0.6, indicating that the myr(−)Gag-mediated inhibition was of a dominant negative nature and not simply due to the dilution of wild-type Gag (Fig. 2E, bottom panel).

Recruitment of nonmyristoylated Gag to membrane and lipid rafts mediated by coexpression with myristoylated Gag. The appearance of the nonmyristoylated Gag in viral particles suggests that the nonmyristoylated Gag was associated with the membrane when coexpressed with the myristoylated Gag, in contrast to the results seen when it was expressed alone. To test this using a more specific method, membrane flotation experiments were carried out using sucrose step gradients. Following Western blotting (Fig. 3, left panel), Gag distribution to membrane-bound and non-membrane-bound fractions was semiquantitated using an image analyzer (Fig. 3, right panel). The initial analysis was performed using a physiological

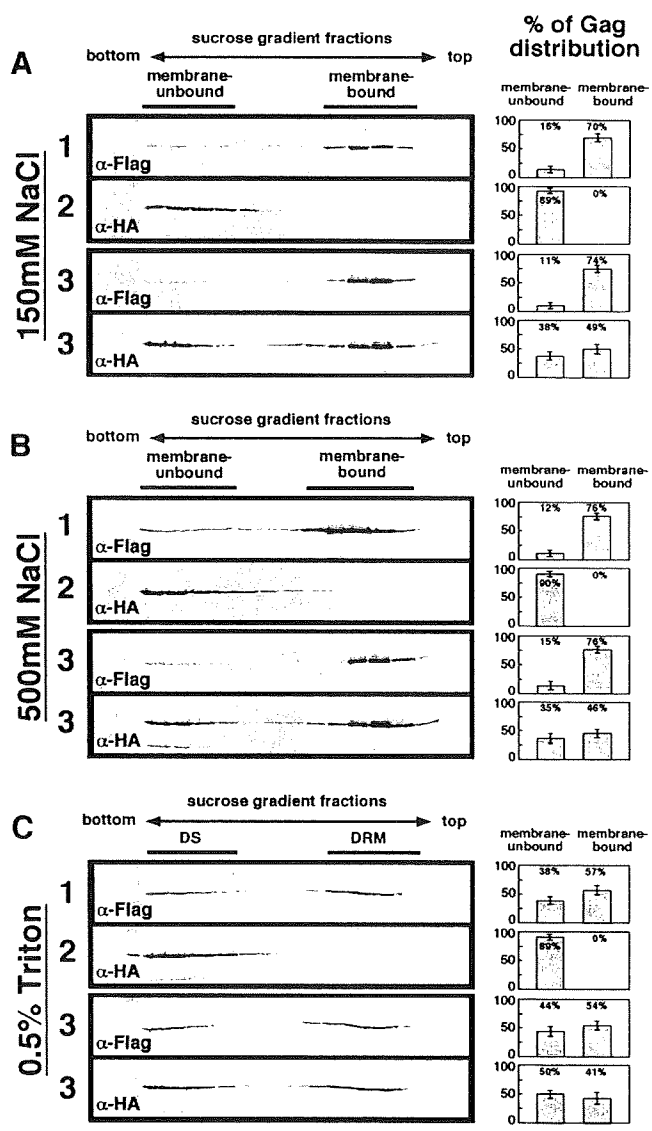

FIG. 3. Membrane and lipid raft associations of Gag. HeLa cells were singly transfected with myr(+)Gag-Flag (panel 1) or myr(−)Gag-HA (panel 2) or were cotransfected with myr(+)Gag-Flag and myr(−)Gag-HA constructs at a 1:1 DNA ratio (panels 3). (A and B) Membrane affinity of Gag. Cells were resuspended in buffer with 150 mM NaCl (A) or 500 mM NaCl (B). Following brief sonication, cell lysates were clarified at 4°C at 2,000 rpm for 5 min. Supernatants were adjusted to 70% (wt/vol) sucrose, layered at the bottom of 70%, 65%, and 10% (wt/vol) sucrose step gradients in PBS, and subjected to equilibrium flotation centrifugation. Fractions of the gradients were subjected to Western blotting using anti-Flag and anti-HA antibodies. Representative blots are shown. (C) Lipid raft association of Gag. Cells were resuspended in buffer with 150 mM NaCl, and following sonication, cell lysates were treated at 4°C with 0.5% Triton X-100 for 10 min. Supernatants were similarly separated in 70%, 65%, and 10% (wt/vol) sucrose step gradients and subjected to Western blotting. Representative blots are shown. All data from three independent experiments were subjected to semiquantitation by an image analyzer, and the percentages of Gag distribution to membrane-bound and non-membrane-bound fractions are shown.

concentration of salt (150 mM NaCl). As expected, the cells expressing the myristoylated Gag alone showed distribution of the majority of Gag to membrane-bound fractions (Fig. 3A, panel 1). In contrast, cells expressing the nonmyristoylated

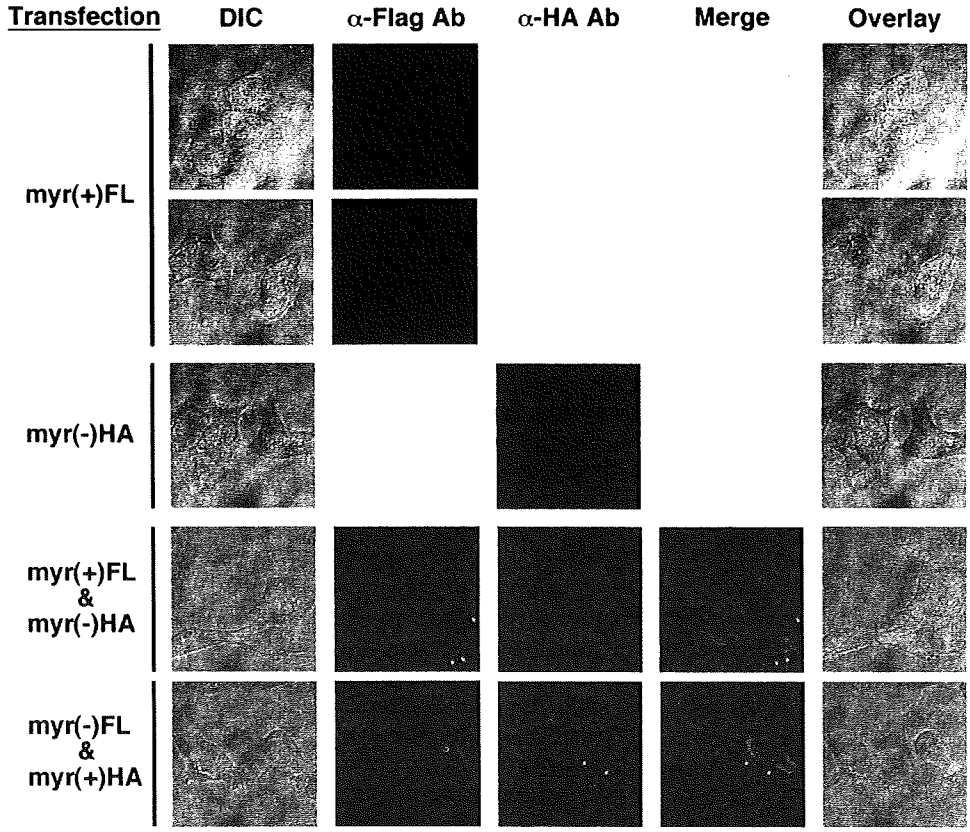

FIG. 4. Intracellular localization of Gag. HeLa cells (in 12-well plates) were singly transfected with myr(+)Gag-Flag or myr(−)Gag-HA or doubly transfected with a combination of myr(+)Gag-Flag and myr(−)Gag-HA or a combination of myr(−)Gag-Flag and myr(+)Gag-HA at a 1:1 DNA ratio. At 2 days posttransfection, cells were immunostained with anti-Flag (shown in green) and anti-HA (shown in red) antibody (Ab). All micrographs are shown at the same magnification. Arrows show Gag accumulation at small areas of the plasma membrane. FL, Flag; DIC, differential interference contrast.

Gag alone showed a complete block in membrane binding (Fig. 3A, panel 2). When the coexpressed cells were analyzed, the myristoylated Gag was detected in membrane-bound fractions at a level similar to that of the myristoylated Gag expressed alone, while the nonmyristoylated Gag was nearly evenly distributed to membrane-bound and non-membrane-bound fractions (Fig. 3A, panels 3). We reasoned that the inefficient incorporation of nonmyristoylated Gag into membrane-bound fractions led to the preferential incorporation of myristoylated Gag into virus particles. The sample preparation was also carried out under high-salt conditions (500 mM NaCl) and subjected to membrane flotation analysis. The treatment caused no alterations in membrane flotation profiles for the myristoylated or nonmyristoylated Gag under single-expression (Fig. 3B, panels 1 and 2) or coexpression (Fig. 3B, panels 3) conditions. These results indicate that approximately one-half (45 to 50%) of the nonmyristoylated Gag population was incorporated into membrane-bound fractions through coassembly with the myristoylated Gag, which did not dissociate under high-salt conditions.

The plasma membrane has been considered to contain a number of microdomains, such as lipid rafts. Lipid rafts are often isolated as membranes insoluble to nonionic detergent, although such detergent-resistant membranes (DRM) may be only an approximation of lipid rafts (8, 19, 27, 29, 33, 38, 62). Recent reports suggest that HIV particle assembly and budding take place at the raft-rich area of the plasma membrane (2, 9, 34, 42, 46). Raft association of Gag was examined by similar equilibrium flotation centrifugation but after 0.5% Triton X-100 treatment on ice. More than one-half of the myristoylated Gag (50 to 60% of total Gag) was distributed to the DRM fractions, suggesting that a large portion of the membrane-bound Gag population was incorporated into raft fractions (Fig. 3C, panel 1). When the coexpressed cells were analyzed, similar fractionation profiles, i.e., distributions to the DRM and detergent-sensitive fractions, were observed for the myristoylated Gag, but the nonmyristoylated Gag was always slightly enriched in the detergent-sensitive fractions (Fig. 3C, panels 3). As expected, the nonmyristoylated Gag alone showed no distribution to DRM (Fig. 3C, panel 2). Altogether, the data indicate that a considerable portion (40 to 50%) of the nonmyristoylated Gag population shifted to the membrane-bound and raft-associated fractions through coassembly with the myristoylated Gag but that associations of the myristoylated Gag with membrane and lipid rafts remained unaffected.

Alterations in Gag distribution by coexpression of nonmyristoylated Gag. Confocal microscopy was carried out to examine the intracellular distribution of each form of Gag (Fig. 4 and Table 1). HeLa cells were transfected with myr(+)Gag-Flag and/or myr(−)Gag-HA and were stained with anti-Flag

TABLE 1. Semiquantitation of Gag distribution patterns[a]

Construct	No. of cells expressed/ no. of cells counted (% transfection efficiency)	No. (%) of cells with:		
		Staining at the PM[b]	Punctate staining in the cytoplasm	Diffuse staining in the cytoplasm
myr(+)Gag	103/138 (75.0)	57 (55.3)	36 (35.0)	10 (9.7)
myr(−)Gag	47/70 (67.1)	0 (0)	0 (0)	47 (100)
myr(+)Gag + myr(−)Gag	60[c]/108 (55.6)	5 (8.3)	42 (70.0)	13 (21.7)

[a] Cells (at 48 h posttransfection) were subjected to confocal microscopy. The numbers of cells in which Gag was observed only in diffuse form in the cytoplasm, accumulated at the PM, or accumulated as cytoplasmic puncta (often accompanied by PM accumulations) were counted.
[b] PM, plasma membrane.
[c] Number of doubly expressed cells.

and/or anti-HA antibodies at 48 h posttransfection. When singly transfected cells were stained with anti-Flag or anti-HA antibody, the majority of myr(+)Gag-Flag-transfected cells showed strong staining on the plasma membrane [myr(+)FL; Fig. 4, upper panel], but in some cells, a diffuse staining alone or cytoplasmic accumulation of a small fraction of Gag was seen in the cytoplasm [myr(+)FL; Fig. 4, lower panel]. The strong staining on the plasma membrane most likely represented particle assembly of myristoylated Gag, whereas the punctate staining in the cytoplasm may correspond to internalized Gag, as reported recently (31). In contrast, only diffuse and smooth cytosolic staining was observed in the myr(−)Gag-HA-transfected cells. When cotransfected cells were stained with anti-Flag and anti-HA antibodies, antigen distributions were not identical to those observed in singly transfected cells. Both forms of Gag were observed in the cytoplasm along with punctate accumulation of the myristoylated Gag in the cytoplasm. The accumulation of myristoylated Gag was also observed at small areas of the plasma membrane (Fig. 4). The punctate accumulation in the cytoplasm was more frequently observed than that in the expression of myristoylated Gag alone. Similar findings were made when a reverse combination of constructs, myr(+)Gag-HA and myr(−)Gag-Flag, was used (Fig. 4, bottom panel). For quantitation, the numbers of cells with these patterns of Gag distribution were counted; the results are summarized in Table 1. Together, the data indicate that upon coexpression with the nonmyristoylated Gag, localization of the wild-type Gag altered to the punctate area in the cytoplasm or accumulated locally at small areas of the plasma membrane.

Accumulation of myristoylated Gag in early and late endosomes. To define the organelle to which the myristoylated Gag was retargeted, the cotransfected cells were doubly stained with anti-Flag antibody [for myr(+)Gag] and antibodies against organelle markers (Fig. 5). The trans-Golgi network marker TGN46 did not colocalize with the Gag accumulated in the cytoplasm. In contrast, partial colocalization with the Gag was observed when Texas Red-conjugated EGF was added to the culture medium to trace the endocytic pathways. Further studies were carried out by using various endosomal markers: Trf (for recycling endosome), EEA1 (for early endosome), Rab7 (for late endosome), CD63 (for late endosome and multivesicular bodies), and LAMP1 (for lysosome). The Gag colocalized with EEA1 but not with Trf, indicating that the Gag was redirected selectively to the early but not the recycling endosome. The Gag also colocalized with Rab7 and partially with CD63. Virtually no colocalization was observed with LAMP1, however. Gag localization at the surrounding area within the perinuclear area has been reported as Gag targeted to endosomes (47). The data indicate that the Gag was distributed to a series of compartments along the endocytic pathways. Expression of the myristoylated Gag alone less frequently showed cytoplasmic accumulation of Gag but showed colocalization similar to that seen with EEA1 and CD63.

Budding arrest and intracellular budding in coexpressed cells. Our results showed that coexpression with the nonmyristoylated Gag resulted in a reduction in particle production and intracellular accumulation of the wild-type Gag in the endosomes. A detailed analysis was carried out by electron microscopy. As shown in Fig. 6A, spherical budding particles with an electron-dense layer, typical of immature HIV particles, were observed at the surface of myr(+)Gag-Flag-transfected cells (in 20 out of 30 cells observed), although they were also seen at intracellular vesicles (7 out of 30 cells observed). Expression of myr(−)Gag-HA showed no particle budding at any site of the cells (Fig. 6B), as is consistent with previous reports (23, 25). When cells cotransfected with plasmids for myr(+)Gag-Flag and myr(−)Gag-HA were similarly analyzed, interconnected virions were observed on the cell surface (13 out of 50 cells observed), which is suggestive of budding arrest (Fig. 6D). Small patches with an electron-dense layer were observed on the cell surface at a low frequency (4 out of 50 cells observed) (Fig. 6C), but normal particle budding was hardly seen (2 out of 50 cells observed). In some cells (18 out of 50 cells observed), vesicles that accommodate spherical particles with an electron-dense layer were also visible, which is suggestive of intracellular budding or internalization of viral particles (Fig. 6E). No interconnected virions were seen in cells transfected with myr(+)Gag-Flag alone. Together, these results suggest that coexpression of the nonmyristoylated form of Gag disrupts the normal transport pathway of Gag and arrests particle budding and release.

Myristoylated Gag relocation to endosomes following accumulation at the plasma membrane in coexpressed cells. To further understand Gag behavior in coexpressed cells, we carried out a temporal study of Gag distribution by confocal microscopy (Fig. 7A). HeLa cells were similarly transfected with myr(+)Gag-Flag and/or myr(−)Gag-HA and stained with anti-Flag and anti-HA antibodies. We observed 100 to 150 Gag-positive cells and counted the numbers of cells showing different Gag distribution patterns (diffuse or punctate in the cytoplasm or accumulated at the plasma membrane) (Fig. 7B). In myr(+)Gag-Flag-transfected cells, diffuse distribution of Gag was evident at an early time point (12 h posttransfection),

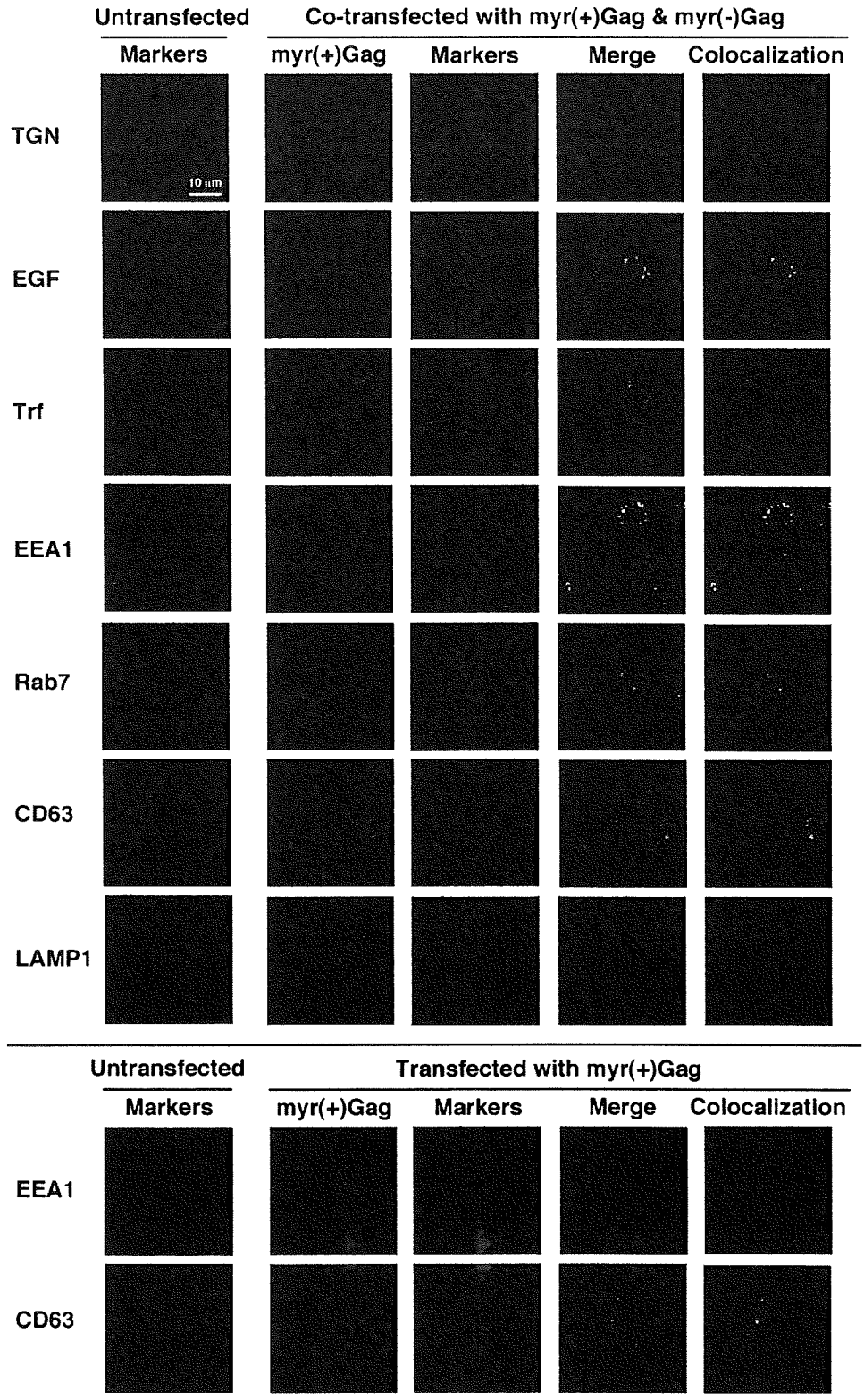

FIG. 5. Colocalization of Gag with organelle markers. HeLa cells (in 12-well plates) were left untransfected (left panel), transfected with myr(+)Gag-Flag alone, or cotransfected with myr(+)Gag-Flag and myr(−)Gag-HA constructs at a 1:1 DNA ratio. Cells were immunostained for myr(+)Gag by anti-Flag antibody (shown in green) and for the following markers: TGN46, EGF, Trf, EEA1, Rab7, CD63, and LAMP1 (shown in red). Colocalization images (right panel) were produced using ImageJ software. All micrographs are shown at the same magnification. Bar, 10 μm.

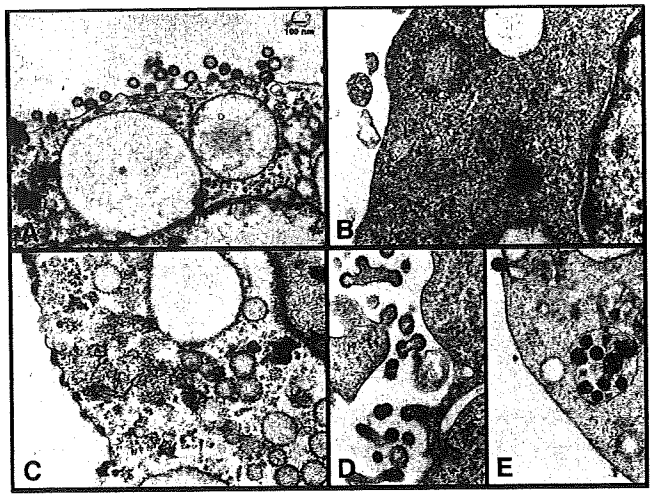

FIG. 6. Electron microscopy. HeLa cells were transfected with myr(+)Gag-Flag and/or myr(−)Gag-HA constructs and were subjected to electron microscopy at 48 h posttransfection. (A) myr(+)Gag-Flag-transfection; (B) myr(−)Gag-HA-transfection; (C to E) cotransfection with myr(+)Gag-Flag and myr(−)Gag-HA at a 1:1 DNA ratio. All micrographs are shown at the same magnification. Bar, 100 nm.

and Gag accumulation at the plasma membrane was clearly seen at late time points (55% of Gag-positive cells at 48 h posttransfection). Punctate staining in the cytoplasm was also observed at late time points but at a lower frequency (35% of Gag-positive cells) than was seen with the plasma membrane staining. As expected, cells transfected with myr(−)Gag-HA showed only diffuse cytosolic staining throughout the period. In coexpressed cells, diffuse distribution of Gag in the cytoplasm predominated at 12 and 24 h posttransfection, and, in contrast, punctate staining became prominent at late time points. Gag accumulation at the plasma membrane only peaked at 36 h posttransfection. The relocation of Gag was apparent for myr(+)Gag but not for myr(−)Gag. Overall, the data are consistent with the possibility that in coexpressed cells, Gag first accumulated at the plasma membrane and then internalized, possibly through endocytosis.

Particle production restored by NC deletion but not by PTAP mutation in nonmyristoylated Gag. Our data indicated that the nonmyristoylated Gag coassembled with the wild-type Gag and inhibited particle budding. If this was the case, deletion of the Gag assembly domain within the nonmyristoylated Gag might restore particle production. We deleted the NC domain that is a major assembly region of Gag within the context of *pol*-deleted pNL43 [referred to as NC(−)] and carried out coexpression experiments using HeLa cells. Western blotting using anti-Flag, anti-HA, and anti-p24CA antibodies showed that intracellular Gag expression results were broadly equivalent for all constructs (Fig. 8A, top panel). HIV particles were collected from culture media by pelleting through sucrose cushions and analyzed by Western blotting (Fig. 8A, middle panel). As reported previously (50), NC deletion in myr(+)Gag did not abolish but moderately reduced particle production (Fig. 8A, lane 3), confirming that NC is not absolutely required for particle production but is responsible for efficient assembly. In the absence of the myristoyl moiety, however, no NC(−)Gag particles were produced (Fig. 8A, lane 6). Coexpression of myr(+)Gag and myr(−)Gag again showed a severe reduction in particle production (Fig. 8A, lane 4). When NC was deleted in the context of myr(−)Gag and the construct was coexpressed with myr(+)Gag [i.e., coexpression of myr(+)Gag and myr(−)NC(−)Gag], particle production was restored (Fig. 8A, lane 5). Semiquantitation revealed that the level of particles produced by the coexpression was nearly equal to that produced by the coexpression of the myr(+)Gag and myr(+)NC(−)Gag constructs (Fig. 8A, bottom panel; compare lanes 2 and 5). These results suggest that a strong Gag-Gag interaction through NC may be necessary for the inhibition by the nonmyristoylated Gag to occur.

We observed budding arrest on the plasma membrane by electron microscopy (Fig. 6D), with results that were somewhat similar to those observed for the defective phenotype of the L domain mutant that fails to recruit TSG101, a host factor involved in particle budding, from the cytoplasm (22, 30, 66). Therefore, we hypothesized that the nonmyristoylated Gag that was not recruited to membranes might have adsorbed TSG101 in the cytoplasm because of its intact L domain and that, as a result, the wild-type Gag failed to bud from the membrane. To this end, we used the L domain mutant [referred to as PTAP(−)] in the *pol*-deleted pNL43 context and carried out coexpression experiments using HeLa cells. Western blotting (Fig. 8A, upper and middle panels) and semiquantitation (Fig. 8A, bottom panels) showed that coexpression of myr(+)Gag and myr(−)PTAP(−)Gag produced only a low level of particles, in similarity to the results seen with coexpression of myr(+)Gag and myr(−)Gag, indicating that the introduction of a PTAP(−) mutation in myr(−)Gag did not reverse the inhibition of particle production (Fig. 8A; compare lanes 10 and 11).

To understand why the NC deletion in myr(−)Gag reversed the inhibition of particle production in coexpression, we carried out coexpression experiments using four different combinations of Gag constructs [i.e., myr(+)Gag-Flag plus myr(+)Gag-HA, myr(+)Gag-Flag plus myr(−)Gag-HA, myr(+)Gag-Flag plus myr(+)NC(−)Gag-HA, and myr(+)Gag-Flag plus myr(−)NC(−)Gag-HA] and compared the membrane affinity characteristics of all of the Gag proteins by membrane flotation analysis. Sample preparation was initially carried out in the presence of 150 mM NaCl (Fig. 8B, upper panel). As expected, Western blotting showed that, in all combinations of Gag constructs used, myr(+)Gag-Flag was detected in membrane-bound fractions, indicating that membrane binding of myr(+)Gag was unaffected by coexpression with either myr(−)Gag or NC(−)Gag constructs. In contrast, coexpressed myr(−)Gag-HA again showed nearly equal distributions to membrane-bound and non-membrane-bound fractions. The deletion of NC in myr(+)Gag-HA did not alter membrane flotation profiles for the Gag protein, and the deletion of NC in the myr(−)Gag-HA context also had no impact on the recruitment of Gag to membranes. Semiquantitation by an image analyzer confirmed these findings (Fig. 8B, right panel). Next, samples were prepared in the presence of 500 mM NaCl and subjected to membrane flotation analysis (Fig. 8B, lower panel). Most of the membrane flotation profiles were essentially similar to the profiles of samples prepared in the presence of 150 mM NaCl. Approximately one-half of the coexpressed myr(−)Gag-HA population (51%) was incorporated into membrane-bound fractions at a level similar to that seen with the same Gag

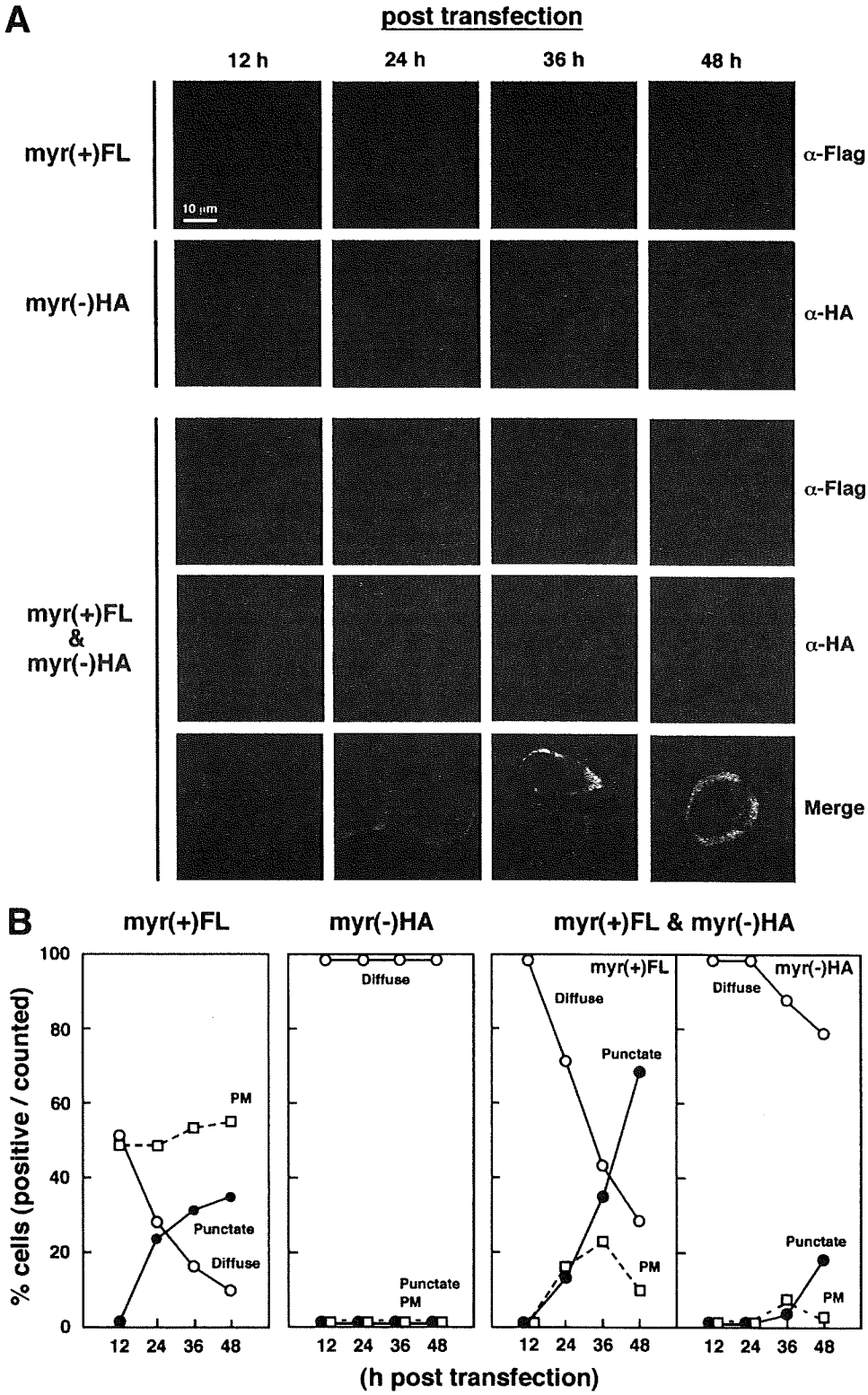

FIG. 7. Temporal study of Gag localization. HeLa cells (in 12-well plates) were singly transfected with myr(+)Gag-Flag or myr(−)Gag-HA or doubly transfected with a combination of myr(+)Gag-Flag and myr(−)Gag-HA at a 1:1 DNA ratio. (A) Confocal images of Gag localization. At 12, 24, 36, and 48 h posttransfection, cells were immunostained for myr(+)Gag by use of anti-Flag antibody (shown in green) and for myr(−)Gag by use of anti-HA antibody (shown in red). Nuclei were stained with TOPRO-3. All micrographs are shown at the same magnification. Bar, 10 μm. (B) Semiquantitation of Gag localization. Gag-positive cells (100 to 150) were observed at each time point, and the numbers of cells with each pattern of Gag distribution (accumulation at the plasma membrane, only diffuse distribution in the cytoplasm, or accumulation at cytoplasmic puncta) were counted.

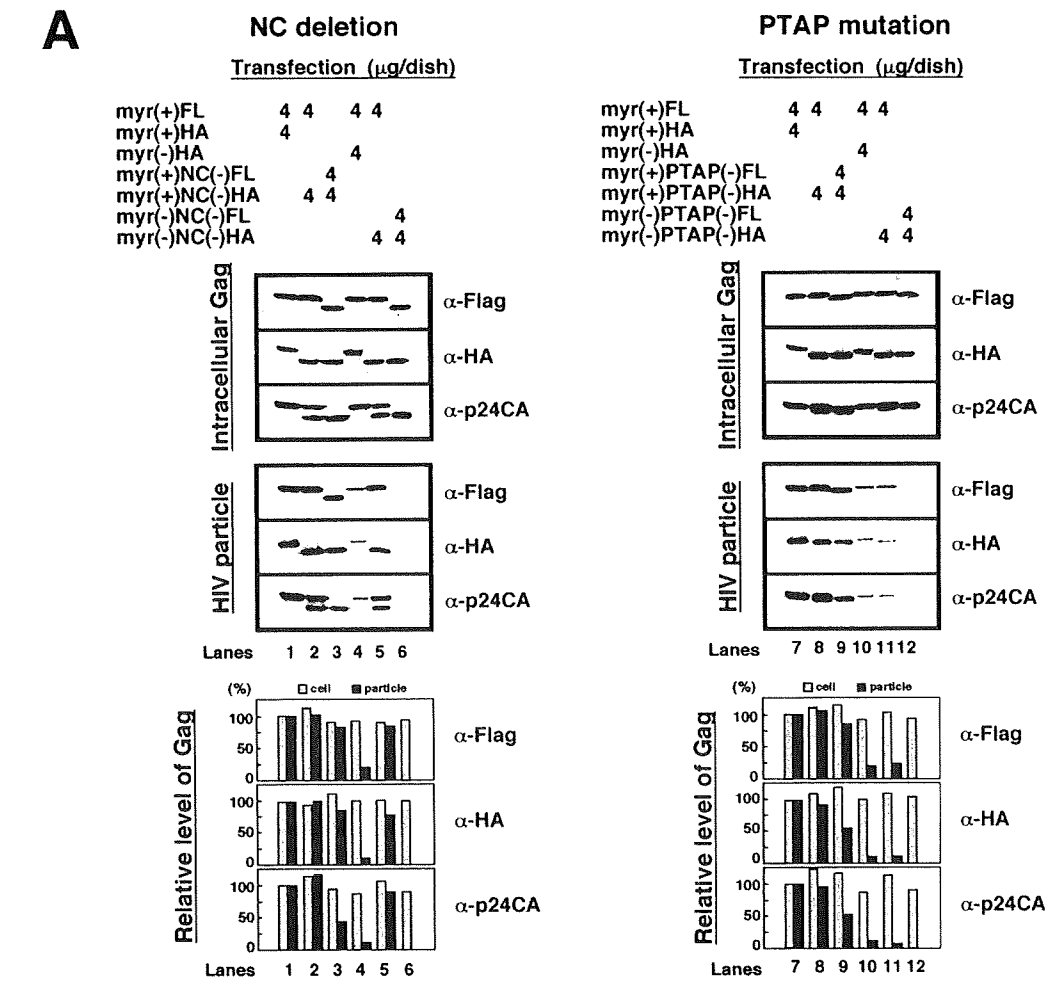
A
NC deletion
Transfection (μg/dish)
myr(+)FL 4 4 4 4
myr(+)HA 4
myr(-)HA 4
myr(+)NC(-)FL 4
myr(+)NC(-)HA 4 4
myr(-)NC(-)FL 4
myr(-)NC(-)HA 4 4
PTAP mutation
Transfection (μg/dish)
myr(+)FL 4 4 4 4
myr(+)HA 4
myr(-)HA 4
myr(+)PTAP(-)FL 4
myr(+)PTAP(-)HA 4 4
myr(-)PTAP(-)FL 4
myr(-)PTAP(-)HA 4 4
Intracellular Gag
HIV particle
α-Flag
α-HA
α-p24CA
Lanes 1 2 3 4 5 6
Lanes 7 8 9 10 11 12
Relative level of Gag
(%)
cell
particle
100
50
0

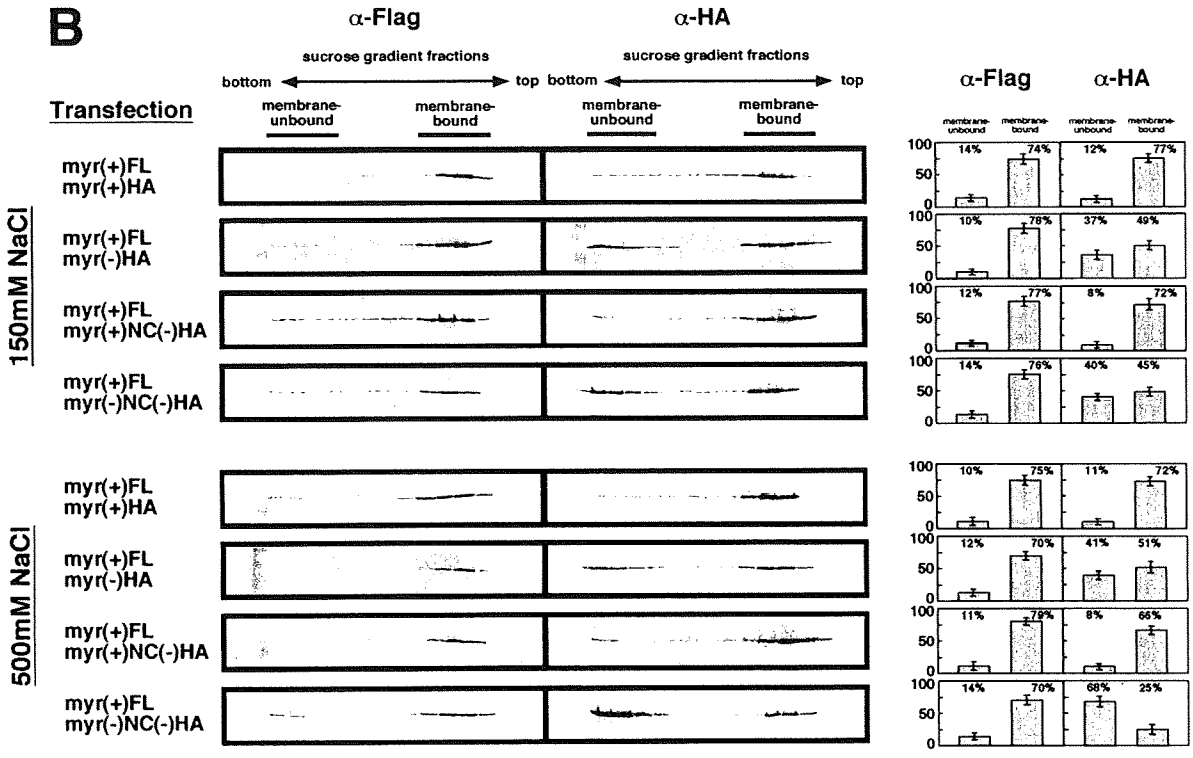
B
α-Flag
α-HA
sucrose gradient fractions
bottom
top
membrane-unbound
membrane-bound
Transfection
150mM NaCl
500mM NaCl
myr(+)FL
myr(+)HA
myr(-)HA
myr(+)NC(-)HA
myr(-)NC(-)HA
14%
74%
12%
77%
10%
78%
37%
49%
12%
77%
8%
72%
14%
76%
40%
45%
10%
75%
11%
72%
12%
70%
41%
51%
11%
79%
8%
66%
14%
70%
68%
25%

analyzed in the presence of 150 mM NaCl (49%). In contrast, when coexpression with myr(−)NC(−)Gag-HA was examined, we found a much larger population of the Gag (68%) dissociated from membrane under high-salt conditions. Together, the data suggest that the deletion of NC in the context of myr(−) Gag did not affect the recruitment of myr(−)Gag to membrane that was mediated by myr(+)Gag but that such myr(−)Gag derivatives became readily dissociated from a membrane-bound Gag complex under high-salt conditions.

Suppression of endosomal localization of Gag by NC deletion but not PTAP mutation in nonmyristoylated Gag. We examined whether the restored particle production was accompanied by Gag localization to the plasma membrane. HeLa cells were cotransfected with the myr(+)Gag-Flag and myr(−)Gag-HA containing the NC deletion or PTAP mutation and were stained with anti-Flag and anti-HA antibodies at 48 h posttransfection (Fig. 9A). We observed approximately 100 Gag-positive cells and evaluated Gag distribution (diffused alone or punctate in the cytoplasm or accumulated at the plasma membrane) as described above (Fig. 9B). Confocal microscopy confirmed that Gag accumulation at the plasma membrane was prominent (50% of Gag-positive cells) and that intracellular accumulation of Gag was not frequent (35% of Gag-positive cells) in myr(+)Gag-transfected cells. In contrast, in cells cotransfected with myr(+)Gag and myr(−)Gag, punctate staining in the cytoplasm was more evident (68% of Gag-positive cells) than staining at the plasma membrane (8% of Gag-positive cells).

Diffuse cytosolic distribution of Gag was often observed in these cells. When myr(+)Gag was coexpressed with myr(−)Gag containing the NC deletion, both forms of Gag were localized predominantly at the plasma membrane (51% of Gag-positive cells) and the punctate staining in the cytoplasm was markedly reduced (33% of Gag-positive cells). A similar pattern was observed for cells cotransfected with myr(+)Gag and myr(+)NC(−)Gag. The results indicate that the deletion of NC within the context of myr(−)Gag allowed Gag to localize to the plasma membrane. It should be noted that, in the cells coexpressing the NC-deleted Gag, the plasma membrane staining was less punctate than that seen in cells expressing the wild-type Gag alone (Fig. 9A). This finding was very apparent in cells expressing myr(+)NC(−)Gag alone (data not shown), suggesting that punctate accumulation of Gag at the plasma membrane may represent Gag-Gag interactions through the NC. In contrast, the introduction of the PTAP mutation into the context of myr(−)Gag did not reverse Gag accumulation to the endosome (58% of Gag-positive cells). Altogether, our results indicate that negative effects of nonmyristoylated Gag on particle production driven by myristoylated Gag are dependent on the presence of NC.

DISCUSSION

In this study, we carried out coexpression experiments using the wild-type and nonmyristoylated Gag proteins of HIV and examined the behaviors of Gag proteins. As is consistent with previous reports (12, 37, 44, 52), we found that nonmyristoylated Gag, which normally has no membrane-binding ability, was partly incorporated into the membrane-bound and lipid raft-associated fractions in the presence of the wild-type Gag. Importantly, our results demonstrated that the coassembly with nonmyristoylated Gag did not affect the membrane and raft affinities of the wild-type Gag (Fig. 3) but severely inhibited the production of viral particles in a dominant negative manner (Fig. 2B and D), suggesting that it might impair other steps in the particle assembly process, such as Gag multimerization, localization, and particle budding.

Previous studies have indicated that progressive C-terminal truncations of Gag that remove Gag-Gag interaction domains resulted in a decrease in the membrane affinity of Gag, suggesting that multimerization of Gag enhanced its membrane affinity (60, 72). The reports are consistent with a myristoyl switch model in which exposure of the N-terminal myristoyl moiety is stabilized in Gag multimer but not in monomeric Gag. Indeed, structural studies have provided evidence that the N-terminal myristoyl moiety was exposed in a MA trimer but sequestered in a MA monomer (64). It is conceivable that multimerization-competent Gag binds membrane more efficiently than multimerization-incompetent Gag partly because the number of the myristoyl moieties per Gag molecule/complex is higher. However, our membrane flotation data showed that, even though a considerable portion of the nonmyristoylated Gag coassembled with the myristoylated Gag, the membrane binding efficiency of the myristoylated Gag was unaffected by the interaction with the nonmyristoylated Gag (Fig. 3), suggesting that at least under the conditions we tested, the efficiency of Gag membrane binding was unlikely to be determined by the number of myristoylated Gags in a Gag complex.

Our deletion experiments showed that the deletion of NC, even in the context of nonmyristoylated Gag, did not reduce the level of Gag incorporation to membrane-bound fractions when it was coexpressed with the wild-type Gag (Fig. 8B), suggesting the possibility that the myr(−)NC(−)Gag may similarly impose a severe negative effect on particle production. In contrast, however, the deletion of NC suppressed the inhibi-

FIG. 8. Viral particle production restored by NC deletion in nonmyristoylated Gag. (A) Intracellular Gag expression and viral particle production. HeLa cells (in 6-cm-diameter dishes) were transfected with myr(+)Gag and/or myr(−)Gag constructs in which the NC or PTAP domain was further deleted. The DNA amounts of the Gag constructs used are indicated at the top of the panel. At 2 days posttransfection, cells were collected (top panels) and culture media were subjected to purification of viral particles by ultracentrifugation (middle panels). The materials were subjected to SDS-PAGE followed by Western blotting using anti-Flag, anti-HA, and anti-HIV-1 p24CA antibodies. The Western blots were subjected to semiquantitation by use of an image analyzer (bottom panels). The levels of Gag obtained in expression of myr(+)FL plus myr(+)HA were set at 100%. (B) Membrane affinity of Gag. HeLa cells were cotransfected with two Gag constructs as indicated at a 1:1 DNA ratio. Cells were resuspended in buffer with 150 mM NaCl (upper panels) or 500 mM NaCl (lower panels) and subjected to equilibrium flotation centrifugation. Fractions of the gradients were subjected to Western blotting using anti-Flag and anti-HA antibodies. Representative blots are shown. All data from three independent experiments were subjected to semiquantitation by use of an image analyzer, and the percentages of Gag distribution to membrane-bound and non-membrane-bound fractions are shown.

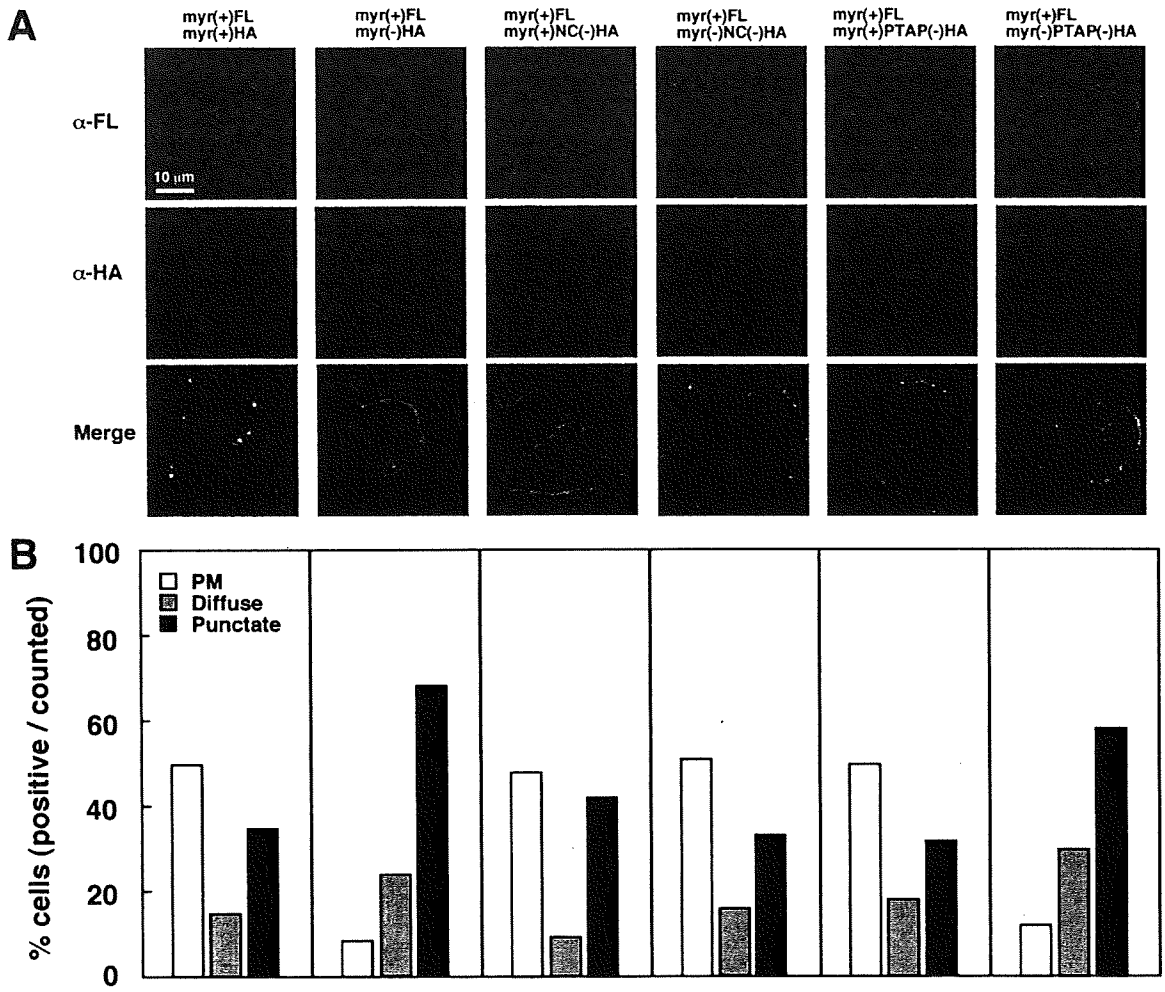

FIG. 9. Suppression of endosomal localization of Gag by NC deletion. HeLa cells (in 12-well plates) were transfected with myr(+)Gag and/or myr(−)Gag constructs in which the NC or PTAP domain was further deleted (indicated at the top panel) at a 1:1 DNA ratio. (A) Confocal images of Gag localization. At 48 h posttransfection, cells were immunostained for myr(+)Gag by anti-Flag antibody (shown in green) and for myr(−)Gag by anti-HA antibody (shown in red). Nuclei were stained with TOPRO-3. (B) Semiquantitation of Gag localization. In each expression experiment, approximately 100 Gag-positive cells were subjected to analysis of Gag distribution patterns. Bars: white, accumulation at the plasma membrane; gray, diffuse distribution alone in the cytoplasm; black, punctate staining in the cytoplasm.

tion of particle production imposed by coexpression with the nonmyristoylated Gag (Fig. 8A). These results indicate that the restoration of particle production was not due to a reduction in the coassembly of Gag, which could have occurred by deletion of NC. Rather, the restoration appeared to be linked to a weaker interaction of myr(−)NC(−)Gag with myr(+)Gag in a Gag complex, which was manifested as the dissociation of myr(−)NC(−)Gag from the Gag complex under high-salt conditions (Fig. 8B). Our data suggest that, when nonmyristoylated Gag is involved, the NC-mediated Gag-Gag interaction might not support proper particle assembly but might rather have a deleterious effect on particle assembly.

In microscopy analysis, diffuse localization of the wild-type Gag increased upon coexpression of the nonmyristoylated Gag (Fig. 4 and 7). This apparently contradicts the membrane flotation data discussed above. As it has been shown that antibody-based detection of nondenatured, full-length Gag is skewed toward preferential detection of non-membrane-bound, cytosolic Gag over membrane-bound Gag multimer (49), it is possible that the immunofluorescence microscopy data are unlikely to represent the efficiency of Gag membrane binding as accurately as the membrane flotation data. It is probable, however, that the diffuse cytosolic staining observed in the coexpressed cells represents Gag associated with small vesicles present in the cytoplasm.

The immunofluorescence microscopy revealed another qualitatively distinct phenotype, i.e., the relocation of Gag to endosomal compartments in cells coexpressing the myristoylated and nonmyristoylated Gag proteins (Fig. 4, 5, and 7). In cell types such as HeLa and T cells, HIV Gag targets to the plasma membrane, where particle assembly occurs (3). However, a number of studies have shown that Gag may also target to endosomes, especially in macrophages, suggesting that such endosomal targeting may be essential for HIV assembly and budding in macrophages (3, 41, 47, 53, 55). Endosomal targeting has been reported for other cell types as well (5, 17, 26, 43, 60, 61). Studies including time-lapse analysis have suggested that Gag is initially targeted to late endosomes and subse-

quently relocates to the plasma membrane (5, 17, 43, 54, 61). Therefore, it is possible that, upon coassembly with the nonmyristoylated Gag, Gag targeting might be shifted from the plasma membrane to the endosomes or that Gag transport from the endosomes to the plasma membrane might be blocked. Recent studies using the inhibitors of the endocytic pathway and membrane-impermeative dyes, however, have suggested that the plasma membrane is the primary site for Gag targeting and assembly even in macrophages and that Gag accumulates at endosomes by internalization from the plasma membrane (16, 31, 69). Such internalization of Gag and nascent virus particles from the plasma membrane to endosomes is even more pronounced when the HIV-1 accessory protein Vpu is defective (28, 39). In the present study, we found, using pNL43-based Vpu-positive constructs expressed in HeLa cells, that coexpression of myristoylated and nonmyristoylated Gag proteins caused aberrant Gag accumulations on the plasma membrane (Fig. 6) and Gag accumulations at early and late endosomes (Fig. 7). We suggest that the most likely scenario would be that (i) the nonmyristoylated Gag was assembled with the wild-type Gag and targeted to the plasma membrane but that (ii) the failure of the further particle assembly process halted particle budding (discussed below) and (iii) the aberrant budding particles were internalized by the endocytic machinery of the host cell. As is consistent with this model, we observed a broad distribution of Gag throughout the endosomal pathways and virus particle accumulation in intracellular compartments. It would be of interest to test whether the use of the inhibitors of the endocytic pathway could rescue the defects imposed by nonmyristoylated Gag.

Somewhat surprisingly, we observed interconnected virions on the plasma membrane when wild-type Gag was coexpressed with its nonmyristoylated counterpart, indicating a defect at a relatively late stage of the particle budding process. A similar defective phenotype was originally described for L domain mutants (15, 24) and has been shown to link with the lack of interaction with TSG101 (21). We observed, however, that deletion of the L domain within the nonmyristoylated Gag did not restore the particle production or reverse the Gag accumulation to endosomes, excluding the possibility that the nonmyristoylated Gag might impair the availability of TSG101. Thus, although the L domain mutations and coexpression of the nonmyristoylated Gag impose similar budding defects, the mechanism by which the nonmyristoylated Gag arrests budding is unlikely to be related to the L domain defect. Interestingly, from studies of Mason-Pfizer monkey virus, a prototype retrovirus for studies of capsid formation prior to plasma membrane targeting, it has been reported that amino acid substitutions in MA that were predicted to inhibit the exposure of the N-terminal myristoyl moiety led to arrest at an early stage of particle formation (63). This budding defect was explained as a result of insufficient affinity of the capsid with the membrane that would otherwise promote wrapping of the capsid by the membrane. Similarly, it is possible that a high molar number of myristoyl moieties may be needed on the membrane-proximal surface of an HIV Gag assembly complex to promote virus particle budding at the plasma membrane. According to this model, if the molar number of myristoyl moieties were not above a threshold due to incorporation of nonmyristoylated Gag molecules into a Gag complex, the complex would not drive the membrane curvature required for particle budding and release. This inhibitory effect likely depends on a tight incorporation of nonmyristoylated Gag into the Gag shell complex underneath the membrane, and the NC deletion that loosens Gag-Gag interaction eliminates the restriction. The defect in virus budding observed in our study is consistent with this hypothesis. Certainly, further study is necessary to elucidate the relationships between Gag membrane binding and virus particle budding. Our study provides a clue to help elucidate this less-studied aspect of retrovirus particle production. As the negative impact of nonmyristoylated Gag on virus assembly by wild-type Gag is substantial, future investigation of the role of Gag-membrane interaction in virus budding may also provide insight into new strategies for antiretroviral therapy.

ACKNOWLEDGMENTS

We thank Eric O. Freed and David E. Ott for the supply of PTAP- and NC-deleted pNL43, respectively.

This work was supported by an AIDS grant from the Ministry of Health, Labor, and Welfare of Japan, by a Grant-in-Aid for Scientific Research from the Japan Society for the Promotion of Science, and by a 21st-century COE Program grant from the Ministry of Education, Culture, Sports, Science and Technology of Japan.

REFERENCES

1. **Adachi, A., S. Koenig, H. E. Gendelman, D. Daugherty, S. Gattoni-Celli, A. S. Fauci, and M. A. Martin.** 1987. Productive, persistent infection of human colorectal cell lines with human immunodeficiency virus. J. Virol. **61**:209–213.
2. **Aloia, R. C., H. Tian, and F. C. Jensen.** 1993. Lipid composition and fluidity of the human immunodeficiency virus envelope and host cell plasma membranes. Proc. Natl. Acad. Sci. USA **90**:5181–5185.
3. **Amara, A., and D. R. Littman.** 2003. After Hrs with HIV. J. Cell Biol. **162**:371–375.
4. **Andrawiss, M., Y. Takeuchi, L. Hewlett, and M. Collins.** 2003. Murine leukemia virus particle assembly quantitated by fluorescence microscopy: role of Gag-Gag interactions and membrane association. J. Virol. **77**:11651–11660.
5. **Basyuk, E., T. Galli, M. Mougel, J. M. Blanchard, M. Sitbon, and E. Bertrand.** 2003. Retroviral genomic RNAs are transported to the plasma membrane by endosomal vesicles. Dev. Cell **5**:161–174.
6. **Berkowitz, R. D., J. Luban, and S. P. Goff.** 1993. Specific binding of human immunodeficiency virus type 1 Gag polyprotein and nucleocapsid protein to viral RNAs detected by RNA mobility shift assays. J. Virol. **67**:7190–7200.
7. **Borsetti, A., A. Ohagen, and H. G. Göttlinger.** 1998. The C-terminal half of the human immunodeficiency virus type 1 Gag precursor is sufficient for efficient particle assembly. J. Virol. **72**:9313–9317.
8. **Brown, D. A., and E. London.** 1998. Structure and origin of ordered lipid domains in biological membranes. J. Membr. Biol. **164**:103–114.
9. **Brügger, B., B. Glass, P. Haberkant, I. Leibrecht, F. T. Wieland, and H. G. Krausslich.** 2006. The HIV lipidome: a raft with an unusual composition. Proc. Natl. Acad. Sci. USA **103**:2641–2646.
10. **Bryant, M., and L. Ratner.** 1990. Myristoylation-dependent replication and assembly of human immunodeficiency virus 1. Proc. Natl. Acad. Sci. USA **87**:523–527.
11. **Bryant, M. L., R. O. Heuckeroth, J. T. Kimata, L. Ratner, and J. I. Gordon.** 1989. Replication of human immunodeficiency virus 1 and Moloney murine leukemia virus is inhibited by different heteroatom-containing analogs of myristic acid. Proc. Natl. Acad. Sci. USA **86**:8655–8659.
12. **Burniston, M. T., A. Cimarelli, J. Colgan, S. P. Curtis, and J. Luban.** 1999. Human immunodeficiency virus type 1 Gag polyprotein multimerization requires the nucleocapsid domain and RNA and is promoted by the capsid-dimer interface and the basic region of matrix protein. J. Virol. **73**:8527–8540.
13. **Dannull, J., A. Surovoy, G. Jung, and K. Moelling.** 1994. Specific binding of HIV-1 nucleocapsid protein to PSI RNA *in vitro* requires N-terminal zinc finger and flanking basic amino acid residues. EMBO J. **13**:1525–1533.
14. **Demirov, D. G., A. Ono, J. M. Orenstein, and E. O. Freed.** 2002. Overexpression of the N-terminal domain of TSG101 inhibits HIV-1 budding by blocking late domain function. Proc. Natl. Acad. Sci. USA **99**:955–960.
15. **Demirov, D. G., J. M. Orenstein, and E. O. Freed.** 2002. The late domain of human immunodeficiency virus type 1 p6 promotes virus release in a cell type-dependent manner. J. Virol. **76**:105–117.

16. **Deneka, M., A. Pelchen-Matthews, R. Byland, E. Ruiz-Mateos, and M. Marsh.** 2007. In macrophages, HIV-1 assembles into an intracellular plasma membrane domain containing the tetraspanins CD81, CD9, and CD53. J. Cell Biol. **177**:329–341.
17. **Dong, X., H. Li, A. Derdowski, L. Ding, A. Burnett, X. Chen, T. R. Peters, T. S. Dermody, E. Woodruff, J. J. Wang, and P. Spearman.** 2005. AP-3 directs the intracellular trafficking of HIV-1 Gag and plays a key role in particle assembly. Cell **120**:663–674.
18. **Dorfman, T., A. Bukovsky, A. Öhagen, S. Höglund, and H. G. Göttlinger.** 1994. Functional domains of the capsid protein of human immunodeficiency virus type 1. J. Virol. **68**:8180–8187.
19. **Edidin, M.** 2003. The state of lipid rafts: from model membranes to cells. Annu. Rev. Biophys. Biomol. Struct. **32**:257–283.
20. **Gamble, T. R., F. F. Vajdos, S. Yoo, D. K. Worthylake, M. Houseweart, W. I. Sundquist, and C. P. Hill.** 1996. Crystal structure of human cyclophilin A bound to the amino-terminal domain of HIV-1 capsid. Cell **87**:1285–1294.
21. **Gamble, T. R., S. Yoo, F. F. Vajdos, U. K. von Schwedler, D. K. Worthylake, H. Wang, J. P. McCutcheon, W. I. Sundquist, and C. P. Hill.** 1997. Structure of the carboxyl-terminal dimerization domain of the HIV-1 capsid protein. Science **278**:849–853.
22. **Garrus, J. E., U. K. von Schwedler, O. W. Pornillos, S. G. Morham, K. H. Zavitz, H. E. Wang, D. A. Wettstein, K. M. Stray, M. Cote, R. L. Rich, D. G. Myszka, and W. I. Sundquist.** 2001. Tsg101 and the vacuolar protein sorting pathway are essential for HIV-1 budding. Cell **107**:55–65.
23. **Gheysen, D., E. Jacobs, F. de Foresta, C. Thiriart, M. Francotte, D. Thines, and M. De Wilde.** 1989. Assembly and release of HIV-1 precursor Pr55*gag* virus-like particles from recombinant baculovirus-infected insect cells. Cell **59**:103–112.
24. **Göttlinger, H. G., T. Dorfman, J. G. Sodroski, and W. A. Haseltine.** 1991. Effect of mutations affecting the p6 gag protein on human immunodeficiency virus particle release. Proc. Natl. Acad. Sci. USA **88**:3195–3199.
25. **Göttlinger, H. G., J. G. Sodroski, and W. A. Haseltine.** 1989. Role of capsid precursor processing and myristoylation in morphogenesis and infectivity of human immunodeficiency virus type 1. Proc. Natl. Acad. Sci. USA **86**:5781–5785.
26. **Grigorov, B., F. Arcanger, P. Roingeard, J. L. Darlix, and D. Muriaux.** 2006. Assembly of infectious HIV-1 in human epithelial and T-lymphoblastic cell lines. J. Mol. Biol. **359**:848–862.
27. **Hancock, J. F.** 2006. Lipid rafts: contentious only from simplistic standpoints. Nat. Rev. Mol. Cell Biol. **7**:456–462.
28. **Harila, K., I. Prior, M. Sjoberg, A. Salminen, J. Hinkula, and M. Suomalainen.** 2006. Vpu and Tsg101 regulate intracellular targeting of the human immunodeficiency virus type 1 core protein precursor Pr55gag. J. Virol. **80**:3765–3772.
29. **Holm, K., K. Weclewicz, R. Hewson, and M. Suomalainen.** 2003. Human immunodeficiency virus type 1 assembly and lipid rafts: $Pr55^{gag}$ associates with membrane domains that are largely resistant to Brij98 but sensitive to Triton X-100. J. Virol. **77**:4805–4817.
30. **Huang, M., J. M. Orenstein, M. A. Martin, and E. O. Freed.** 1995. p6Gag is required for particle production from full-length human immunodeficiency virus type 1 molecular clones expressing protease. J. Virol. **69**:6810–6818.
31. **Jouvenet, N., S. J. Neil, C. Bess, M. C. Johnson, C. A. Virgen, S. M. Simon, and P. D. Bieniasz.** 2006. Plasma membrane is the site of productive HIV-1 particle assembly. PLoS Biol. **4**:e435.
32. **Langner, C. A., J. K. Lodge, S. J. Travis, J. E. Caldwell, T. Lu, Q. Li, M. L. Bryant, B. Devadas, G. W. Gokel, G. S. Kobayashi, and J. I. Gordon.** 1992. 4-oxatetradecanoic acid is fungicidal for *Cryptococcus neoformans* and inhibits replication of human immunodeficiency virus I. J. Biol. Chem. **267**:17159–17169.
33. **Lichtenberg, D., F. M. Goni, and H. Heerklotz.** 2005. Detergent-resistant membranes should not be identified with membrane rafts. Trends Biochem. Sci. **30**:430–436.
34. **Lindwasser, O. W., and M. D. Resh.** 2001. Multimerization of human immunodeficiency virus type 1 Gag promotes its localization to barges, raft-like membrane microdomains. J. Virol. **75**:7913–7924.
35. **Lindwasser, O. W., and M. D. Resh.** 2002. Myristoylation as a target for inhibiting HIV assembly: unsaturated fatty acids block viral budding. Proc. Natl. Acad. Sci. USA **99**:13037–13042.
36. **Martin-Serrano, J., T. Zang, and P. D. Bieniasz.** 2001. HIV-1 and Ebola virus encode small peptide motifs that recruit Tsg101 to sites of particle assembly to facilitate egress. Nat. Med. **7**:1313–1319.
37. **Morikawa, Y., S. Hinata, H. Tomoda, T. Goto, M. Nakai, C. Aizawa, H. Tanaka, and S. Omura.** 1996. Complete inhibition of human immunodeficiency virus Gag myristoylation is necessary for inhibition of particle budding. J. Biol. Chem. **271**:2868–2873.
38. **Munro, S.** 2003. Lipid rafts: elusive or illusive? Cell **115**:377–388.
39. **Neil, S. J., S. W. Eastman, N. Jouvenet, and P. D. Bieniasz.** 2006. HIV-1 Vpu promotes release and prevents endocytosis of nascent retrovirus particles from the plasma membrane. PLoS Pathog. **2**:e39.
40. **Nelle, T. D., and J. W. Wills.** 1996. A large region within the Rous sarcoma virus matrix protein is dispensable for budding and infectivity. J. Virol. **70**:2269–2276.
41. **Nguyen, D. G., A. Booth, S. J. Gould, and J. E. Hildreth.** 2003. Evidence that HIV budding in primary macrophages occurs through the exosome release pathway. J. Biol. Chem. **278**:52347–52354.
42. **Nguyen, D. H., and J. E. Hildreth.** 2000. Evidence for budding of human immunodeficiency virus type 1 selectively from glycolipid-enriched membrane lipid rafts. J. Virol. **74**:3264–3272.
43. **Nydegger, S., M. Foti, A. Derdowski, P. Spearman, and M. Thali.** 2003. HIV-1 egress is gated through late endosomal membranes. Traffic **4**:902–910.
44. **Ono, A., D. Demirov, and E. O. Freed.** 2000. Relationship between human immunodeficiency virus type 1 Gag multimerization and membrane binding. J. Virol. **74**:5142–5150.
45. **Ono, A., and E. O. Freed.** 1999. Binding of human immunodeficiency virus type 1 Gag to membrane: role of the matrix amino terminus. J. Virol. **73**:4136–4144.
46. **Ono, A., and E. O. Freed.** 2001. Plasma membrane rafts play a critical role in HIV-1 assembly and release. Proc. Natl. Acad. Sci. USA **98**:13925–13930.
47. **Ono, A., and E. O. Freed.** 2004. Cell-type-dependent targeting of human immunodeficiency virus type 1 assembly to the plasma membrane and the multivesicular body. J. Virol. **78**:1552–1563.
48. **Ono, A., J. M. Orenstein, and E. O. Freed.** 2000. Role of the Gag matrix domain in targeting human immunodeficiency virus type 1 assembly. J. Virol. **74**:2855–2866.
49. **Ono, A., A. A. Waheed, A. Joshi, and E. O. Freed.** 2005. Association of human immunodeficiency virus type 1 Gag with membrane does not require highly basic sequences in the nucleocapsid: use of a novel Gag multimerization assay. J. Virol. **79**:14131–14140.
50. **Ott, D. E., L. V. Coren, E. N. Chertova, T. D. Gagliardi, K. Nagashima, R. C. Sowder II, D. T. Poon, and R. J. Gorelick.** 2003. Elimination of protease activity restores efficient virion production to a human immunodeficiency virus type 1 nucleocapsid deletion mutant. J. Virol. **77**:5547–5556.
51. **Paillart, J. C., and H. G. Göttlinger.** 1999. Opposing effects of human immunodeficiency virus type 1 matrix mutations support a myristyl switch model of gag membrane targeting. J. Virol. **73**:2604–2612.
52. **Park, J., and C. D. Morrow.** 1992. The nonmyristylated $Pr160^{gag-pol}$ polyprotein of human immunodeficiency virus type 1 interacts with $Pr55^{gag}$ and is incorporated into viruslike particles. J. Virol. **66**:6304–6313.
53. **Pelchen-Matthews, A., B. Kramer, and M. Marsh.** 2003. Infectious HIV-1 assembles in late endosomes in primary macrophages. J. Cell Biol. **162**:443–455.
54. **Perlman, M., and M. D. Resh.** 2006. Identification of an intracellular trafficking and assembly pathway for HIV-1 gag. Traffic **6**:731–745.
55. **Raposo, G., M. Moore, D. Innes, R. Leijendekker, A. Leigh-Brown, P. Benaroch, and H. Geuze.** 2002. Human macrophages accumulate HIV-1 particles in MHC II compartments. Traffic **3**:718–729.
56. **Reicin, A. S., S. Paik, R. D. Berkowitz, J. Luban, I. Lowy, and S. P. Goff.** 1995. Linker insertion mutations in the human immunodeficiency virus type 1 *gag* gene: effects on virion particle assembly, release, and infectivity. J. Virol. **69**:642–650.
57. **Rein, A., M. R. McClure, N. R. Rice, R. B. Luftig, and A. M. Schultz.** 1986. Myristylation site in Pr65gag is essential for virus particle formation by Moloney murine leukemia virus. Proc. Natl. Acad. Sci. USA **83**:7246–7250.
58. **Saermark, T., A. Kleinschmidt, A. M. Wulff, H. Andreassen, A. Magee, and V. Erfle.** 1991. Characterization of N-myristoyl transferase inhibitors and their effect on HIV release. AIDS **5**:951–958.
59. **Sakaguchi, K., N. Zambrano, E. T. Baldwin, B. A. Shapiro, J. W. Erickson, J. G. Omichinski, G. M. Clore, A. M. Gronenborn, and E. Appella.** 1993. Identification of a binding site for the human immunodeficiency virus type 1 nucleocapsid protein. Proc. Natl. Acad. Sci. USA **90**:5219–5223.
60. **Sandefur, S., V. Varthakavi, and P. Spearman.** 1998. The I domain is required for efficient plasma membrane binding of human immunodeficiency virus type 1 $Pr55^{Gag}$. J. Virol. **72**:2723–2732.
61. **Sherer, N. M., M. J. Lehmann, L. F. Jimenez-Soto, A. Ingmundson, S. M. Horner, G. Cicchetti, P. G. Allen, M. Pypaert, J. M. Cunningham, and W. Mothes.** 2003. Visualization of retroviral replication in living cells reveals budding into multivesicular bodies. Traffic **4**:785–801.
62. **Simons, K., and E. Ikonen.** 1997. Functional rafts in cell membranes. Nature **387**:569–572.
63. **Stansell, E., E. Tytler, M. R. Walter, and E. Hunter.** 2004. An early stage of Mason-Pfizer monkey virus budding is regulated by the hydrophobicity of the Gag matrix domain core. J. Virol. **78**:5023–5031.
64. **Tang, C., E. Loeliger, P. Luncsford, I. Kinde, D. Beckett, and M. F. Summers.** 2004. Entropic switch regulates myristate exposure in the HIV-1 matrix protein. Proc. Natl. Acad. Sci. USA **101**:517–522.
65. **Tashiro, A., S. Shoji, and Y. Kubota.** 1989. Antimyristoylation of the gag proteins in the human immunodeficiency virus-infected cells with N-myristoyl glycinal diethylacetal resulted in inhibition of virus production. Biochem. Biophys. Res. Commun. **165**:1145–1154.
66. **VerPlank, L., F. Bouamr, T. J. LaGrassa, B. Agresta, A. Kikonyogo, J. Leis, and C. A. Carter.** 2001. Tsg101, a homologue of ubiquitin-conjugating (E2) enzymes, binds the L domain in HIV type 1 $Pr55^{Gag}$. Proc. Natl. Acad. Sci. USA **98**:7724–7729.

67. **von Schwedler, U. K., T. L. Stemmler, V. Y. Klishko, S. Li, K. H. Albertine, D. R. Davis, and W. I. Sundquist.** 1998. Proteolytic refolding of the HIV-1 capsid protein amino-terminus facilitates viral core assembly. EMBO J. **17**:1555–1568.
68. **Wang, C. T., H. Y. Lai, and J. J. Li.** 1998. Analysis of minimal human immunodeficiency virus type 1 *gag* coding sequences capable of virus-like particle assembly and release. J. Virol. **72**:7950–7959.
69. **Welsch, S., O. T. Keppler, A. Habermann, I. Allespach, J. Krijnse-Locker, and H. G. Krausslich.** 2007. HIV-1 buds predominantly at the plasma membrane of primary human macrophages. PLoS Pathog. **3**:e36.
70. **Wills, J. W., C. E. Cameron, C. B. Wilson, Y. Xiang, R. P. Bennett, and J. Leis.** 1994. An assembly domain of the Rous sarcoma virus Gag protein required late in budding. J. Virol. **68**:6605–6618.
71. **Zhou, W., L. J. Patent, J. W. Wills, and M. D. Resh.** 1994. Identification of a membrane-binding domain within the amino-terminal region of human immunodeficiency virus type 1 Gag protein which interacts with acidic phospholipids. J. Virol. **68**:2556–2569.
72. **Zhou, W., and M. D. Resh.** 1996. Differential membrane binding of the human immunodeficiency virus type 1 matrix protein. J. Virol. **70**:8540–8548.

SOCS1 is an inducible host factor during HIV-1 infection and regulates the intracellular trafficking and stability of HIV-1 Gag

Akihide Ryo[a,b,c], Naomi Tsurutani[d], Kenji Ohba[b,e], Ryuichiro Kimura[e,f], Jun Komano[b], Mayuko Nishi[a], Hiromi Soeda[a], Shinichiro Hattori[b], Kilian Perrem[g], Mikio Yamamoto[h], Joe Chiba[f], Jun-ichi Mimaya[i], Kazuhisa Yoshimura[j], Shuzo Matsushita[j], Mitsuo Honda[b], Akihiko Yoshimura[k], Tatsuya Sawasaki[l], Ichiro Aoki[a], Yuko Morikawa[d], and Naoki Yamamoto[b,c]

[a]Department of Pathology, Yokohama City University School of Medicine, 3-9 Fuku-ura, Kanazawa-ku, Yokohama 236-0004, Japan; [b]AIDS Research Center, National Institute of Infectious Diseases, 1-23-1 Toyama, Shinjuku-ku, Tokyo 162-8640, Japan; [d]Kitasato Institute for Life Sciences, Kitasato University, Shirokane 5-9-1, Minato-ku, Tokyo 108-8641, Japan; [e]Department of Molecular Virology, Graduate School of Medicine, Tokyo Medical and Dental University, 1-5-45 Yushima, Bunkyo-ku, Tokyo 113-8519, Japan; [f]Molecular Oncology Laboratory, Department of Pathology, Royal College of Surgeons in Ireland, Smurfit Building, Beaumont Hospital, Dublin 9, Ireland; [h]Department of Biochemistry II, National Defense Medical College, 3-2 Namiki, Tokorozawa-shi, Saitama 359-8513, Japan; [g]Department of Biological Science and Technology, Science University of Tokyo, 2641 Yamazaki, Noda, Chiba 278-8510, Japan; [i]Division of Hematology and Oncology, Shizuoka Children's Hospital, 860 Urushiyama, Aoi-ku, Shizuoka 420-8660, Japan; [j]Division of Clinical Retrovirology and Infectious Diseases, Center for AIDS Research, Graduate School of Medical Sciences, Kumamoto University, Kumamoto 860-0811, Japan; [k]Division of Molecular and Cellular Immunology, Medical Institute of Bioregulation, Kyushu University, Fukuoka 812-8582, Japan; and [l]Cell Free Science and Research Center, Ehime University, Ehime 790-8577, Japan

Edited by Robert C. Gallo, University of Maryland, Baltimore, MD, and approved November 19, 2007 (received for review May 24, 2007)

Human immunodeficiency virus type 1 (HIV-1) utilizes the macromolecular machinery of the infected host cell to produce progeny virus. The discovery of cellular factors that participate in HIV-1 replication pathways has provided further insight into the molecular basis of virus–host cell interactions. Here, we report that the suppressor of cytokine signaling 1 (SOCS1) is an inducible host factor during HIV-1 infection and regulates the late stages of the HIV-1 replication pathway. SOCS1 can directly bind to the matrix and nucleocapsid regions of the HIV-1 p55 Gag polyprotein and enhance its stability and trafficking, resulting in the efficient production of HIV-1 particles via an IFN signaling-independent mechanism. The depletion of SOCS1 by siRNA reduces both the targeted trafficking and assembly of HIV-1 Gag, resulting in its accumulation as perinuclear solid aggregates that are eventually subjected to lysosomal degradation. These results together indicate that SOCS1 is a crucial host factor that regulates the intracellular dynamism of HIV-1 Gag and could therefore be a potential new therapeutic target for AIDS and its related disorders.

AIDS | pathogenesis | drug target | lysozyme

Human immunodeficiency virus type 1 (HIV-1) infection is a multistep and multifactorial process mediated by a complex series of virus–host cell interactions (1, 2). The molecular interactions between host cell factors and HIV-1 are vital to our understanding of not only the nature of the resulting viral replication, but also the subsequent cytopathogenesis that occurs in the infected cells (3). The characterization of the genes in the host cells that are up- or down-regulated upon HIV-1 infection could therefore provide a further elucidation of virus–host cell interactions and identify putative molecular targets for the HIV-1 replication pathway (4).

The HIV-1 p55 Gag protein consists of four domains that are cleaved by the viral protease concomitantly with virus release. This action generates the mature Gag protein comprising the matrix (MA/p17), capsid (CA/p24), nucleocapsid (NC/p7), and p6 domains, in addition to two small spacer peptides, SP1 and SP2 (5, 6). The N-terminal portion of MA, which is myristoylated, facilitates the targeting of Gag to the plasma membrane (PM), whereas CA and NC promote Gag multimerization. p6 plays a central role in the release of HIV-1 particles from PM by interacting with the vacuolar sorting protein Tsg101 and AIP1/ALIX (7–9). Several recent studies have implicated the presence of host factors in the control of the intracellular trafficking of Gag. AP-3δ is a recently characterized endosomal adaptor protein that binds directly to the MA region of Gag and enhances its targeting to the multivesicular body (MVB) during the early stages of particle assembly (10). The *trans*-Golgi network (TGN)-associated protein hPOSH plays another role in Gag transport by facilitating the egress of Gag cargo vesicles from the TGN, where it assembles with envelope protein (Env) before transport to PM (11). Although the involvement of these host proteins in the regulation of intracellular Gag trafficking has been proposed, the detailed molecular mechanisms underlying this process are still not yet well characterized.

In our current work, we demonstrate that the suppressor of cytokine signaling 1 (SOCS1) directly binds HIV-1 Gag and facilitates the intracellular trafficking and stability of this protein, resulting in the efficient production of HIV-1 particles. These results indicate that SOCS1 is a crucial host factor for efficient HIV-1 production and could be an intriguing molecular target for future treatment of AIDS and related diseases.

Results

SOCS1 Is Induced upon HIV-1 Infection and Facilitates HIV-1 Replication via Posttranscriptional Mechanisms. We and others have shown that HIV-1 infection can alter cellular gene expression patterns, resulting in the modification of viral replication and impaired homeostasis in the host cells (4, 12). Hence, to elucidate further the genes and cellular pathways that participate in HIV-1 replication processes, we performed serial analysis of gene expression (SAGE) using either a HIV-1 or mock-infected human T cell line, MOLT-4 (12). Further detailed analysis of relatively low-abundance SAGE tags identified *SOCS1* as a preferentially up-regulated gene after HIV-1 infection. This finding was validated by both semiquantitative RT-PCR and immunoblotting analysis with anti-SOCS1 anti-

Author contributions: A.R. and N.T. contributed equally to this work; A.R., A.Y., Y.M., and N.Y. designed research; A.R., N.T., K.O., R.K., M.N., H.S., S.H., T.S., I.A., and Y.M. performed research; J.K., S.H., M.Y., J.C., J.-i.M., K.Y., S.M., M.H., and A.Y. contributed new reagents/analytic tools; A.R., N.T., K.O., M.N., H.S., K.P., M.Y., K.Y., S.M., T.S., I.A., Y.M., and N.Y. analyzed data; and A.R., K.P., and N.Y. wrote the paper.

The authors declare no conflict of interest.

This article is a PNAS Direct Submission.

Freely available online through the PNAS open access option.

To whom correspondence may be addressed. E-mail: aryo@nih.go.jp or nyama@nih.go.jp.

This article contains supporting information online at www.pnas.org/cgi/content/full/0704831105/DC1.

www.pnas.org/cgi/doi/10.1073/pnas.0704831105

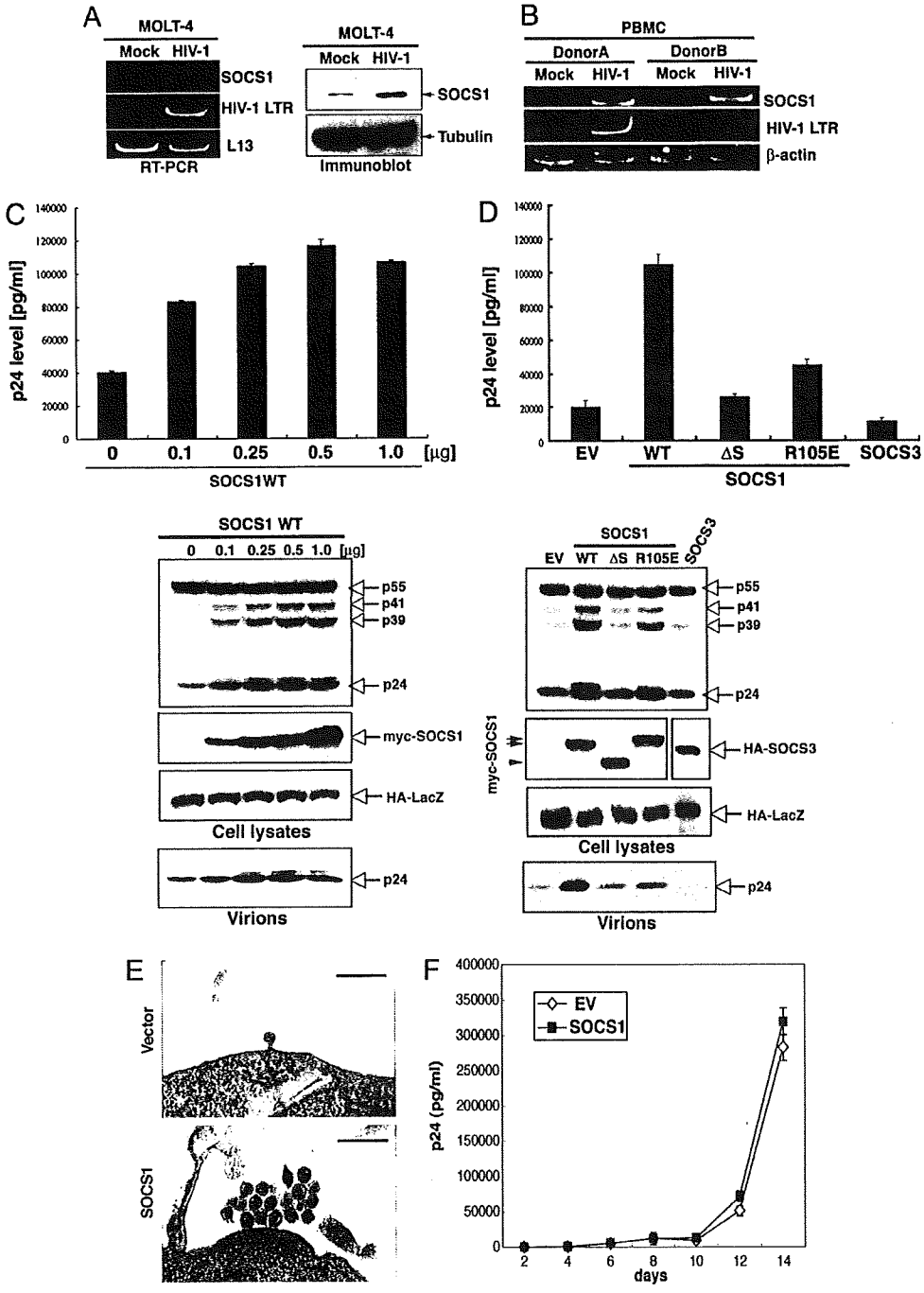

Fig. 1. SOCS1 is induced upon HIV-1 infection and enhances HIV-1 particle production. (*A*) MOLT-4 cells were mock-infected or infected with HIV-1_{NL4-3}, and then total RNA and protein extracts derived from these cells were subjected to semiquantitative RT-PCR (*Left*) and immunoblotting (*Right*), respectively. (*B*) PBMC from two healthy individuals were infected with HIV-1_{NL4-3} or were mock-infected, and SOCS1 expression was examined by semiquantitative RT-PCR. (*C*) 293T cells were transfected with pNL4-3 and cotransfected with various amounts of pcDNA-myc-SOCS1. Forty eight hours after transfection, p24 antigen release into the supernatant in each case was measured by antigen-capture ELISA (*Upper*), and the cell lysates and pelleted viruses were analyzed by immunoblotting (*Lower*). The data shown represent the mean ± SD from three independent experiments. HA-LacZ is a transfection control. (*D*) 293T cells were transfected with pNL4-3 and cotransfected with control vector, SOCS1 (WT), SOCS1ΔS (ΔSOCS box), SOCS1R105E, or SOCS3. Cell lysates and pelleted viruses were then collected after 48 h and subjected to ELISA (*Upper*) or immunoblotting (*Lower*), as described in C. (*E*) 293T cells cotransfected with either pNL4-3 plus control vector, or pNL4-3 plus myc-tagged SOCS1 were analyzed by TEM. Note that substantial numbers of mature virus particles can be observed in the myc-SOCS1-transfected cells. (Scale bars: 500 nm.) (*F*) Jurkat cells were infected with virions (adjusted by p24 levels) from either control vector (EV)- or SOCS1-transfected 293T cells. Supernatant p24 levels at the indicated time points were measured by ELISA.

bodies (Fig. 1*A*). In addition, *SOCS1* was found to be up-regulated also in peripheral blood mononuclear cells (PBMC) from two different individuals (following HIV infection, Fig. 1*B*).

Our initial findings that SOCS1 is induced upon HIV-1 infection prompted us to examine whether this gene product affects viral replication. We first cotransfected 293T cells with a HIV-1 infectious molecular clone, pNL4-3 (13), and also pcDNA-myc-SOCS1, and then monitored the virus production levels in the resulting supernatant. We then performed ELISA using an anti-p24 antibody and found that wild-type SOCS1 significantly increases the production of HIV-1 in the cell supernatant in a dose-dependent manner (Fig. 1*C Upper*). In contrast, neither the SH2 domain-defective mutant (R105E) nor the SOCS box deletion mutant (ΔS) of SOCS1 could promote virus production to the same levels as wild type, indicating that both domains are required for this enhancement (Fig. 1*D Upper*). Furthermore, another SOCS box protein, SOCS3, failed to augment HIV-1 replication in a parallel experiment (Fig. 1*D Upper*), indicating that the role of SOCS1 during HIV-1 replication is specific.

We next performed immunoblotting analysis using cell lysates and harvested virus particles in further parallel experiments (Fig. 1 *C* and *D Lower*). Consistent with our ELISA analysis, the expres-

MICROBIOLOGY

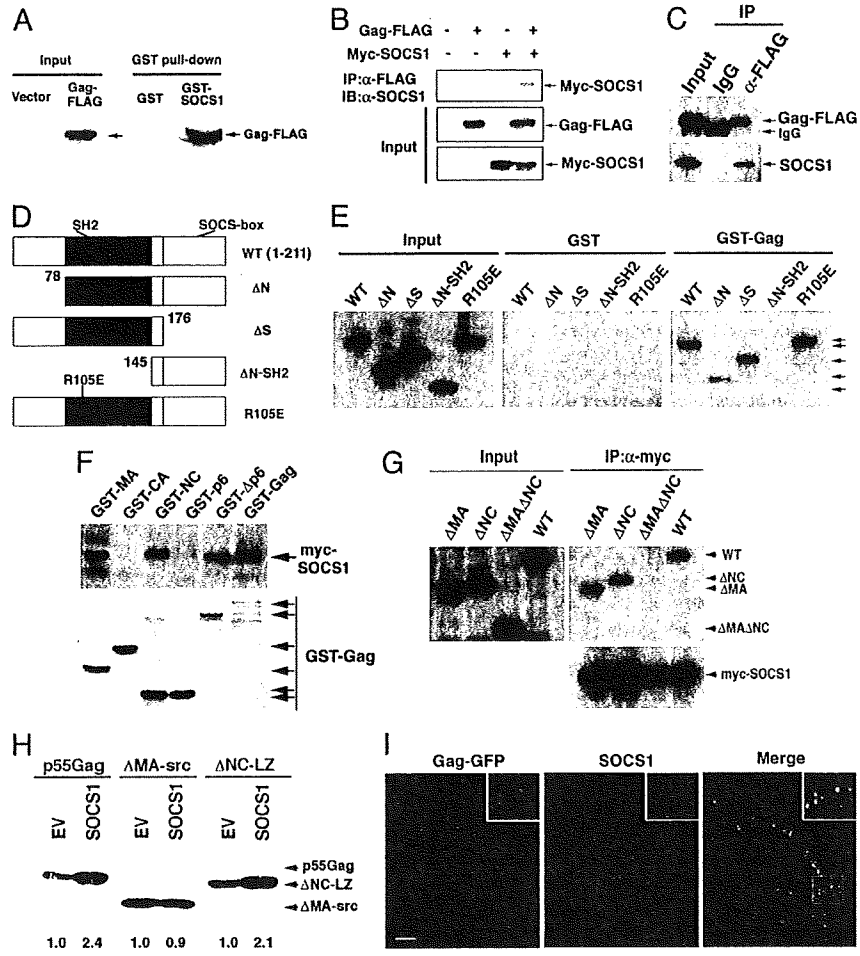

Fig. 2. SOCS1 interacts with HIV-1 Gag. (*A*) Extracts of 293T cells transfected with either empty vector or Gag-FLAG were subjected to pull-down analyses using glutathione–agarose beads with GST-SOCS1 in the presence of 10 ng/ml RNase followed by immunoblotting with anti-FLAG antibodies. (*B*) Extracts of 293T cells transiently expressing myc-SOCS1 and Gag-FLAG were subjected to immunoprecipitation (IP) with anti-FLAG monoclonal antibodies in the presence of 10 ng/ml RNase followed by immunoblotting (IB) analysis with either anti-FLAG or anti-myc polyclonal antibodies. (*C*) 293T cells were transiently transfected with Gag-FLAG, and cell lysates were then subjected to immunoprecipitation with anti-FLAG antibodies followed by immunoblotting with an antibody directed against endogenous SOCS1. (*D* and *E*) 293T cells expressing various myc-tagged SOCS1 mutants (schematically depicted in *D*) were analyzed by GST pull-down analysis with either GST or GST-Gag recombinant protein (*E*). (*F*) GST fusion proteins of the indicated regions of Gag were bound to glutathione beads and incubated with cell lysates from 293T cells expressing myc-SOCS1 in the presence of 10 ng/ml RNase followed by immunoblotting with anti-myc antibodies. (*G*) SOCS1 binds p55 Gag via either its MA or NC domains. 293T cells were transfected with myc-SOCS1 and cotransfected with Gag-FLAG, GagΔMA-FLAG, GagΔNC-FLAG, or GagΔMAΔNC-FLAG. At 24 h after transfection, cell lysates treated with 10 μg/ml RNase were subjected to coimmunoprecipitation with anti-myc monoclonal antibodies followed by immunoblotting with anti-FLAG or anti-myc polyclonal antibodies. (*H*) Functional interaction of SOCS1 with MA but not NC. 293T cells were transfected with wild-type Gag, ΔMA-src, or ΔNC-LZ (Z_{IL}-p6) and cotransfected with either control vector or SOCS1. Supernatant virus particles were then collected after 24 h and subjected to immunoblotting with anti-p24 antibody. Numerical values below the blots indicate fold induction of supernatant p55 signal intensities derived by densitometry. (*I*) Colocalization of SOCS1 with Gag. HeLa cells were transiently transfected with Gag-GFP. After 24 h, the cells were fixed, permeabilized, and immunostained with anti-SOCS1 polyclonal antibody followed by fluorescently labeled secondary antibodies before confocal microscopy. (Scale bar: 10 μm.)

sion of wild-type SOCS1, but neither its SH2 nor SOCS box mutant counterparts, resulted in a marked and dose-dependent increase in the level of intracellular Gag protein, particularly in the case of CA (p24) and intermediate cleavage products corresponding to MA-CA (p41) and CA-NC (p39). This increase was found to be accompanied by an enhanced level of HIV-1 particle production in the supernatant (Fig. 1 *C* and *D Lower*). These results together indicated that SOCS1 facilitates HIV-1 particle production in infected cells and that this role of SOCS1 requires the function of both its SH2 and SOCS box domains. For further details about SOCS1 interaction with MA and NC and SOCS1-enhanced particle production, see supporting information (SI) *Text*.

To examine the morphological aspects of HIV-1 particle production, transmission electron microscopy (TEM) was performed. 293T cells that had been cotransfected with pNL4-3, and either a control vector or a SOCS1 expression construct, were subjected to TEM analysis after fixation in glutaraldehyde. In SOCS1-transfected cells, a significantly increased number of mature virus particles was observed on the surfaces of PM compared with the control vector-transfected cells (Fig. 1*E*). There were also no obvious malformations of the virus particles in SOCS1-expressing cells, such as doublet formation or tethering to PM, which are characteristic of particle budding arrest (14) (Fig. 1*E*). Consistent with this observation, virions from SOCS1-transfected cells were found to be infectious as control viruses in Jurkat cells when the same amounts of virus were infected (Fig. 1*F*). These results together indicate that SOCS1 enhances mature and infectious HIV-1 particle formation.

To elucidate the specific step in HIV-1 production that is enhanced by SOCS1, we next performed gene reporter assays using either luciferase expression constructs under the control of wild-type HIV-LTR (pLTR-luc), or a full-length provirus vector (pNL4-3-luc) (15). Interestingly, SOCS1 overexpression was found not to affect the transcription of these reporter constructs (data not shown), indicating that SOCS1 enhances HIV-1 replication via posttranscriptional mechanisms during virus production.

SOCS1 Interacts with the HIV-1 Gag Protein. The results of our initial experiments indicated that SOCS1 enhances HIV-1 production via a posttranscriptional mechanism. We therefore next tested whether SOCS1 could bind directly to HIV-1 Gag. GST pull-down analysis using C-terminal FLAG-tagged p55 Gag (codon-optimized) and GST-fused SOCS1 revealed that p55 Gag undergoes specific coprecipitation with GST-SOCS1 (Fig. 2*A*). Furthermore, both ectopically expressed myc-tagged SOCS1 and endogenous SOCS1 were found to undergo coimmunoprecipitation with Gag-FLAG in 293T cells (Fig. 2 *B* and *C*). Additionally, GST pull-down analysis with various SOCS1 mutants, as depicted in Fig. 2*D*, further demonstrated that a mutant lacking the both N-terminal and SH2 domain (ΔN-SH2) could not bind

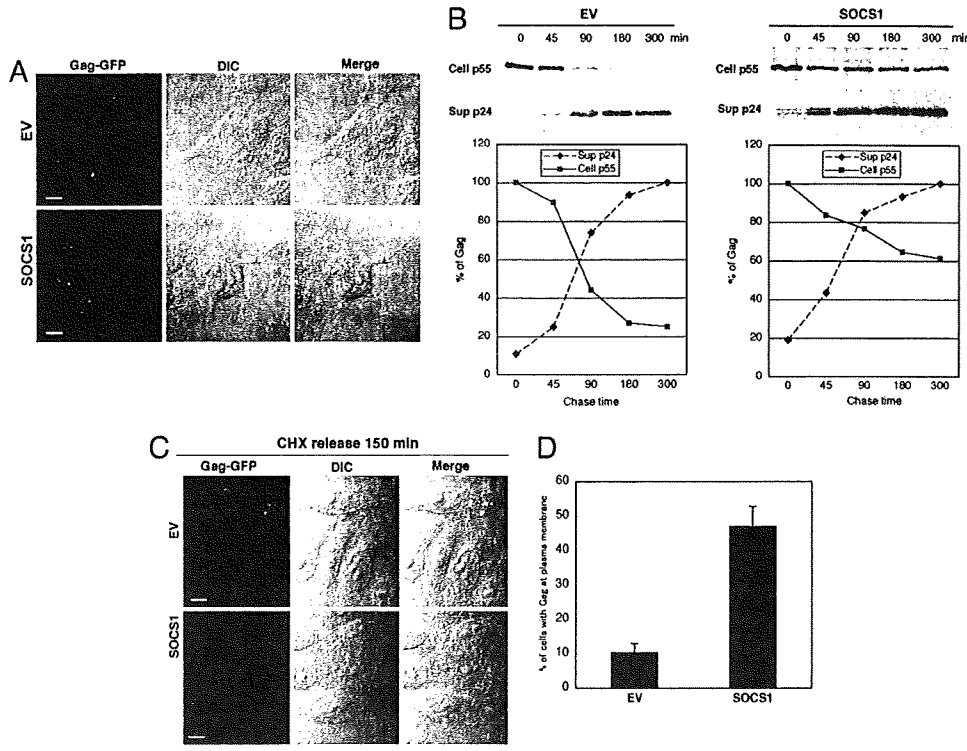

Fig. 3. SOCS1 enhances both the stability and trafficking of HIV-1 Gag. (*A*) HeLa cells cotransfected with pNL4-3 and either control vector (EV) or SOCS1 were immunostained with antibodies targeting anti-p24 (CA). Confocal microscopy with differential interference contrast (DIC) was then performed. (Scale bars: 10 μm.) (*B*) 293T cells were transfected with either a control empty vector (EV) (*Left*) or myc-SOCS1 (*Right*) and cotransfected with pNL4-3. After 48 h, cells were pulse-labeled with [^{35}S]methionine or [^{35}S]cysteine for 15 min and chased for the durations indicated. Cell lysates and pelleted supernatant virions were immunoprecipitated with anti-p24 antibodies followed by autoradiography. (*C* and *D*) HeLa cells seeded on poly-L-lysine-coated cover slides were transfected with either vector control or SOCS1. After 24 h, cells were again transfected with Gag-GFP for 3 h and then treated with 100 μg/ml CHX for 5 h to inhibit protein synthesis. This treatment was followed by incubation with fresh medium; then 150 min after the CHX release, cells were fixed and subjected to confocal microscopy (*C*). (Scale bars: 10 μm.) Cells with Gag protein on the plasma membrane were scored out of 200 transfected cells (*D*).

p55 Gag, whereas an N-terminal or a SOCS box deletion did not affect the binding of SOCS1 to Gag in 293T cells (Fig. 2*E*). This finding indicates that the SH2 domain is important for the interaction of SOCS1 with HIV-1 Gag. Interestingly, the R105E mutant of SOCS1, which disrupts the function of the SH2 domain, still binds Gag (Fig. 2*E*), indicating that the Gag–SOCS1 association is independent of the tyrosine phosphorylation of Gag, as is the case for both HPV-E7 and Vav (16, 17).

To elucidate the SOCS1-binding region of the Gag protein, GST pull-downs with various GST-fused Gag domain constructs were performed. SOCS1 was detected in glutathione bead precipitates with GST-wild-type Gag, GST-Δp6, GST-MA, and GST-NC, but not with other domain constructs (Fig. 2*F*), indicating that SOCS1 interacts with Gag via its MA and NC domains. Consistent with these results, the deletion of both the MA and NC domains of p55 Gag (ΔMAΔNC) completely abolishes its interaction with SOCS1 in coimmunoprecipitation experiments (Fig. 2*G*). Furthermore, *in vitro* analysis with purified proteins also demonstrated that SOCS1 can indeed interact with both the MA and NC regions of HIV-1 Gag in the absence of nucleic acids or other proteins (SI Fig. 5).

We next wished to determine the functional interaction domain in HIV-1 Gag through which SOCS1 functions in terms of virus-like particle production. To this end, we used a MA-deleted Gag mutant with an N-terminal myristoyl tag derived from src (ΔMA-src) (18) and also an NC-deleted Gag mutant with a GCN4 leucine zipper in place of NC, which we herein denote as ΔNC-LZ but which has been described as Z_{IL}-p6 (19). Both of these mutants have been shown still to assemble and bud (18, 19). We found that SOCS1 overexpression can still augment the particle formation of both wild-type Gag and ΔNC-LZ but not ΔMA-src (Fig. 2*H*), indicating that the functional interaction between SOCS1 and HIV-1 Gag is in fact mediated through MA.

To confirm further the direct interaction between SOCS1 and Gag in cells, we examined the intracellular localization of these two proteins. Confocal microscopy revealed that endogenous SOCS1 forms dotted filamentous structures in the cytoplasm and that Gag localizes in a very punctate pattern with SOCS1 from the perinuclear regions to the cell periphery (Fig. 2*I*). These data indicate that SOCS1 interacts with HIV-1 Gag in the cytoplasm during HIV-1 particle production.

SOCS1 Promotes both the Stability of Gag and Its Targeting to the Plasma Membrane. Because we had found from our initial data that SOCS1 increases HIV-1 particle production as a result of its direct interaction with intracellular Gag proteins, we next addressed whether SOCS1 positively regulates Gag stability and subsequent trafficking to PM. Our immunofluorescent analysis with the anti-p24 (CA) antibody initially revealed that SOCS1 overexpression increases the levels of Gag at PM when cotransfected with pNL4-3 at 48 h after transfection, although it was detected at PM in both control and SOCS1-expressing cells (Fig. 3*A*). Furthermore, the levels of cytoplasmic Gag were found to be much lower in the SOCS1-expressing cells compared with the control cells (Fig. 3*A*). These results indicate that SOCS1 enhances Gag trafficking to PM.

To examine next whether SOCS1 affects the stability and trafficking of newly synthesized Gag proteins, we performed pulse–chase analysis. This experiment revealed that SOCS1 significantly increases the stability of the intracellular p55 Gag polyprotein as well as the levels of p24 in the supernatant (Fig. 3*B*). Importantly, p24 was detectable at an earlier time point and reached maximum levels in a shorter period in the cell supernatant of SOCS1-transfected cells compared with control vector-transfected cells (Fig. 3*B*). This finding again suggests that SOCS1 facilitates the intracellular trafficking of newly synthesized Gag proteins to PM.

To confirm this hypothesis further, we performed cycloheximide (CHX) analysis with HeLa cells transfected using either vector control or SOCS1. After 24 h, cells were again transfected with Gag-GFP for 3 h and treated with CHX for 5 h to inhibit protein synthesis. Cells were then cultured in fresh medium without CHX for an additional 150 min and subjected to confocal microscopy. At